Biomass burning emissions of trace gases and particles in marine air at Cape Grim, Tasmania.

S.J. Lawson[1], M.D. Keywood[1], I.E. Galbally[1], J.L. Gras[1], J.M. Cainey[1,2], M.E. Cope[1], P.B. Krummel[1], P.J. Fraser[1], L.P. Steele[1], S.T. Bentley[†], C.P Meyer[1], Z. Ristovski[3] and A.H. Goldstein[4]

[1]{Commonwealth Scientific and Industrial Research Organisation, Oceans and Atmosphere, Aspendale, Australia}

[2]{formerly from the Bureau of Meteorology, Smithton, Tasmania, Australia}

[3]{International Laboratory for Air Quality & Health, Queensland University of Technology, Brisbane, Australia}

[4]{Department of Civil and Environmental Engineering, University of California, Berkeley}

Correspondence to: S. J. Lawson (sarah.lawson@csiro.au)

Abstract

Biomass burning (BB) plumes were measured at the Cape Grim Baseline Air Pollution Station during the 2006 Precursors to Particles campaign, when emissions from a fire on nearby Robbins Island impacted the station. Measurements made included non methane organic compounds (NMOCs) (PTR-MS), particle number size distribution, condensation nuclei (CN) > 3 nm, black carbon (BC) concentration, cloud condensation nuclei (CCN) number, ozone (O_3), methane (CH_4), carbon monoxide (CO), hydrogen (H_2), carbon dioxide (CO_2), nitrous oxide (N_2O), halocarbons and meteorology.

During the first plume strike event (BB1), a four hour enhancement of CO (max ~2100 ppb), BC (~1400 ng m^{-3}) and particles > 3 nm (~13,000 cm^{-3}) with dominant particle mode of 120 nm were observed overnight. A wind direction change lead to a dramatic reduction in BB tracers and a drop in the dominant particle mode to 50 nm. The dominant mode increased in size to 80 nm over 5 hours in calm sunny conditions, accompanied by an increase in ozone. Due to an enhancement in BC but not CO during particle growth, the presence of BB emissions during this period could not be confirmed.

The ability of particles > 80 nm (CN80) to act as CCN at 0.5% supersaturation was investigated. The ΔCCN/ΔCN80 ratio was lowest during the fresh BB plume (56±8%), higher during the particle growth period (77±4%) and higher still (104±3%) in background marine air. Particle size distributions indicate that changes to particle chemical composition, rather than particle size, are driving these changes. Hourly average CCN during both BB events were between 2000-5000 CCN cm^{-3}, which were enhanced above typical background levels by a factor of 6-34, highlighting the dramatic impact BB plumes can have on CCN number in clean marine regions.

During the 29 hours of the second plume strike event (BB2) CO, BC and a range of NMOCs including acetonitrile and hydrogen cyanide (HCN) were clearly enhanced and some enhancements in O_3 were observed ($\Delta O_3/\Delta CO$ 0.001-0.074). A shortlived increase in NMOCs by a factor of 10 corresponded with a large CO enhancement, an increase of the NMOC/CO emission ratio (ER) by a factor of 2 – 4 and a halving of the BC/CO ratio. Rainfall on Robbins Island was observed by radar during this period which likely resulted in a lower fire combustion efficiency, and higher emission of compounds associated with smouldering. This highlights the importance of relatively minor meterological events on BB emission ratios.

Emission factors (EF) were derived for a range of trace gases, some never before reported for Australian fires, (including hydrogen, phenol and toluene) using the carbon mass balance method. This provides a unique set of EF for Australian coastal heathland fires. Methyl halide EFs were higher than EF reported from other studies in Australia and the Northern Hemisphere which is likely due to high halogen content in vegetation on Robbins Island.

This work demonstrates the substantial impact that BB plumes can have on the composition of marine air, and the significant changes that can occur as the plume interacts with terrestrial, aged urban and marine emission sources.

1 Introduction

Biomass burning (BB) is the largest global source of primary carbonaceous fine aerosols and the second largest source of trace gases (Akagi et al., 2011). Species directly emitted from fires include carbon dioxide (CO_2), methane (CH_4), carbon monoxide (CO), nitrogen oxides (NO_x), ammonia (NH_3), non methane organic compounds (NMOCs), carbonyl sulfide (COS), sulfur dioxide (SO_2) and elemental and organic carbonaceous and sulphate-containing particles (Keywood et al., 2011). Secondary species that are formed from BB precursors include ozone (O_3), oxygenated NMOCs and inorganic and organic aerosol (OA). The complex mixture of reactive gases and aerosol that make up BB plumes can act as short lived climate forcers (Keywood et al., 2011). While BB plumes often have the greatest impact on the atmopshere close to the source of the fire, once injected into the free troposphere plumes may travel long distances, so that climate and air quality affects may be regional or even global. A recent modelling study by Lewis et al., (2013) for example highlighted the large contribution that BB emissions make to the burden of several NMOC in the background atmosphere, particularly in the Southern Hemisphere.

With some studies predicting that future changes to the climate will result in increasing fire frequency (Keywood et al., 2011), it is essential to understand the composition of fresh plumes, how they vary temporally and spatially, and the way in which the chemical composition is transformed with aging. This will provide the process understanding to allow models to more accurately predict regional air quality impacts and long term climate affects of BB.

Characterising BB plumes is challenging for several reasons, and significant knowledge gaps still exist. BB plumes contain extremely complex mixtures of trace gases and aerosols, which vary substantially both spatially and temporally. The initial composition of BB plumes is dependent on the combustion process and efficiency of combustion, which has a complex relationship with environmental variables. Combustion efficiency (CE) is a measure of the fraction of fuel carbon completely oxidised to CO_2. However it is difficult to measure all the carbon species required to calculate CE, and so modified combustion efficiency (MCE), which closely approximates the CE, is often used instead, where MCE = $\Delta CO_2/(\Delta CO+\Delta CO_2)$ (Ferek et al., 1998) where Δ refers to excess or above-background quantities. The efficiency of fire combustion depends on fuel size, density and spacing, fuel moisture content, local meteorology (including temperature, windspeed and precipitation), and terrain (van Leeuwen and van der Werf, 2011), and MCE can vary substantially spatially and temporally within one fire. The EF of trace gas and aerosol species are in many cases strongly tied to the efficiency of combustion. Species such as CO, organic carbon, and NMOCs tend to be emitted at higher rates in smouldering fires which burn with low MCE (i.e. have a negative relationship with MCE), while other species such as CO_2 and black carbon (BC) are emitted at higher rates in flaming fires with higher MCE (e.g. have a positive relationship with MCE) (Andreae and Merlet, 2001).

Once emitted, the composition of BB plumes can change very rapidly, with destruction of highly reactive species, coagulation of particles, and formation of secondary species such as O_3, oxygenated NMOCs and secondary organic and inorganic aerosol occuring on a timescale of minutes to hours (Akagi et al., 2012; Vakkari et al., 2014). Particles typically become more oxygenated, and particle size often increases as primary particles are coated either with low-volatility oxidation products of co-emited organic and inorganic gases, or with co-emited semi volatile primary organics (Sahu et al., 2012; Akagi et al., 2012; Vakkari et al., 2014). Changes that occur in the composition of the plume can be highly variable and drivers of variability are difficult to quantify. One example is the large variability in the net OA enhancement in aged BB plumes, with studies reporting both enhancements and decreases in the OA/CO ratio with plume aging (Yokelson et al., 2009; Hennigan et al., 2011; Cubison et al., 2011; Akagi et al., 2012; Hecobian et al., 2012).

While BB is recognised as a major source of CCN (Andreae et al., 2002), the hygroscopicity of fresh BB particles varies enormously from weakly to highly hygroscopic and fuel type appears to be a major driver of the variability (Pratt et al., 2011; Engelhart et al., 2012; Petters et al., 2009) along with particle morphology (Martin et al., 2013). As particles age, in addition to becoming larger, they also generally become more hygroscopic and more easily activated to CCN. However, this is dependent on the initial composition and hygroscopicity of the particle, as well as the hygroscopicity of the coating material (Martin et al., 2013; Engelhart et al., 2012). Most studies of CCN in BB plumes to date have been chamber studies, and there are few ambient studies which have examined the ability of BB particles to act as CCN in fresh and aged plumes.

Ozone is typically destroyed by reaction with nitric oxide (NO) in close proximity to the fire, however once the plume is diluted, O_3 enhancement is often observed (typically normalised to CO). In a recent summary of a number of studies, the enhancement of O_3 to CO typically increases with the age of the plume (Jaffe and Wigder, 2012). However there is significant variation in O_3 enhancements observed between studies which is thought to be dependent on several factors such as precursor emissions (resulting from fuel and combustion efficiency), meteorology, the aerosol affect on plume chemistry and radiation, and photochemical reactions. Many challenges remain in modelling the transformation processes that occur in BB plumes, such as O_3 formation and changes to particle properties, in part due to a lack of high-quality real-time observations (Jaffe and Wigder, 2012; Akagi et al., 2012).

In recent years there have been a number of intensive field and laboratory studies which have characterised both fresh emissions and aged BB emissions. However there are several regions of the globe where BB emissions, including emission factors (EF), have been sparsely characterised. For example, EF data has been published for only a few trace gases in the temperate forests of Southern Australian (Volkova et al., 2014; Paton-Walsh et al., 2012; Paton-Walsh et al., 2005; Paton-Walsh et al., 2014; Paton-Walsh et al., 2008). The lack of Australian temperate EF was evident in a recent compilation of EF by Akagi et al (2011), in which all temperate EF reported were from the Northern Hemisphere (NH) from mostly coniferous forests. Species emitted during combustion can be strongly dependent on vegetation type (e.g. Simpson et al 2011), and EFs from NH coniferous forests are unlikely to be representative of for example Australia's temperate dry sclerophyll forests. Using EF from boreal and tropical forest fires to model BB plumes in temperate regions adds uncertainty to the model outcomes (Akagi et al., 2011), and more detailed chemical measurements of BB plumes in the Southern Hemisphere temperate regions are needed.

An increasingly wide range of sophisticated instruments are being used to measure the trace gas and aerosol composition and microphysical properties in BB plumes. This has lead to a higher proportion of NMOC being quantified than ever. Despite this, there is significant evidence that a large proportion of NMOCs in BB plumes are still not being identified. A compilation of NMOC measurements from 71 laboratory fires using a range of techniques, found that the mass of unidentified NMOC was significant (up to 50%) (Yokelson et al., 2013), though recent work using high-resolution proton transfer reaction – time of flight – mass spectrometry (PTR-TOF-MS) has allowed at least tentative identification of up to 93% of NMOC (Stockwell et al., 2015). Flow reactor experiments have indicated the mass of OA formed in aged BB plumes exceeds the mass of known NMOC precursors, suggesting unknown NMOC precursors, and/or highlighting the important contribution of semi and intermediate volatile species to the increase in OA observed (Ortega et al., 2013). Inclusion of unidentified semi volatile organics in a recent photochemical modelling study of young BB plumes allowed successful simulation of O_3 and OA, if reasonable assumptions were made about the chemistry of the unidentified organics (Alvarado et al., 2015).

Finally, with increasing global population and urbanisation, it is likely that BB events will increasingly impact human settlements, either through close proximity of fires or transport of plumes to urban areas. Consequently a greater understanding is needed of the interactions between BB and urban emissions. These interactions are complex and have not been significantly studied to date, although there is evidence that interactions between these two sources may significantly change the resulting processes and products in plume aging. For example Jaffe and Wigder (2012), Wigder et al., (2013) and Akagi et al., (2013) show that O_3 formation is enhanced when NO_x-limited BB plumes mix with NO_x- rich urban emissions.

Deposition of nitrogen-containing pollutants from major urban areas may also enhance emission of NO_x and other nitrogen containing trace gases in BB plumes (Yokelson et al., 2007). Hecobian et al (2012) found higher concentrations of inorganic aerosol components in aged BB plumes that had mixed with urban emissions compared to BB plumes, which were attributed to higher degree of oxidative processing in the mixed plumes.

In this study we have investigated the chemical composition of fresh BB plumes in marine air at the Cape Grim Baseline Air Pollution Station. The BB event occurred unexpectedly during the Precursors to Particles campaign (Cainey et al., 2007), which aimed to investigate new particle formation in clean marine air. Despite the opportunistic nature of this work and lack of targeted BB measurements, a wide variety of trace gas and aerosol species were quantified which provide valuable information on the composition of BB plumes in this sparsely studied region of the world.

2 Methods

2.1 Cape Grim station location and location of fire

The Cape Grim Baseline Air Pollution Station is located near the north-west tip of the island state of Tasmania, Australia, 40.7° S latitude and 144.7° E longitude (see Fig 1). The station is situated on top of a cliff 94 m above mean sea level. When the wind blows from the south west sector (the Roaring Forties) the air that impacts the station is defined as Baseline and typically has back trajectories over the Southern Ocean of several days. In northerly wind directions, urban air from the city of Melbourne some 300 km away is transported across the ocean (Bass Strait) to the station. North west Tasmania has a mild temperate climate, with average February temperatues of 15±2º C , RH 75±12%, windspeed of 9±4 m s^{-1} (where ±is 1 std dev) and 25 mm precipitation.

From 30 January to 24 February 2006 (the Austral late summer), the Precursors to Particles (P2P) campaign was undertaken (Cainey et al., 2007). On the 15th of February 2006, in the middle of P2P, a fire was ignited on nearby Robbins Island, which lies across farmland 20km east of Cape Grim. Robbins Island (9748 ha) is separated from the Tasmanian mainland by a tidal passage 2km across, and has been a freehold property used for the grazing of sheep and cattle since the 1830s (Buckby, 1988). The vegetation consists of grazed pastures and native vegetation, mostly disturbed coastal heathland (largely endemic *Epacridaceae, Leptospermum*) and woodland (*Leptospermum, Melaleuca* and *Eucalyptus nitida)* with shrubs interspersed by tussock grasses (Poa spp) and sedges (Kitchener and Harris, 2013). The fire burned 2000 ha, mostly coastal heath, over a period of 2 weeks. The vegetation burned is comparable in structure to the mid and lower story vegetation in Australian temperate forest and savannah woodland, though lacks the coarse woody debris and the dominant upper story of trees found particularly in temperate Australian forests. On two occasions an easterly wind advected the BB plume directly to the Cape Grim Station. The first plume strike (BB1) occured from 02:00 – 06:00 (Australian Eastern Standard Time - AEST) on the 16th February, with light easterly winds of 3 m s^{-1} and temperature of 13 ºC and RH of 96 %. The second, more prolonged plume strike (BB2) occurred from 23:00 on 23rd February to 05:00 on the 25th February, with strong easterly winds ranging from 10-16 m s^{-1}, temperatures of 16-22 ºC and RH from 75-95 %.

2.2 Measurements

During P2P, a number of additional instruments were deployed to run alongside the routine measurements. All the measurements made during BB1 and BB2 (routine and P2P measurements) are listed in Table 1, with references supplied for further information. Some additional information is provided here. All levels of trace gases are expressed as volume mixing ratios. As the focus of P2P was clean marine air, PM2.5 and PM10 filter samples were not collected during the BB events.

2.2.1 NMOCs (PTR-MS)

Details on PTR-MS measurements are given in Galbally et al (2007) and some additional information is provided here.

The PTR-MS ran with inlet and drift tube temperature of 75ºC, 600V drift tube, 2.2 mbar drift tube pressure, which equates to an energy field of 140 Td. The O_2^+ signal was ~2% of the primary ion H_3O^+ signal. The PTR-MS ran in multiple ion detection (MID) mode in which 26 masses were selected. Masses included in this work were identified by reviewing instrument intercomparison studies of BB plumes (Christian et al., 2004; Karl et al., 2007b; de Gouw and Warneke, 2007; Stockwell et al., 2015). Protonated masses were identified as m/z 28 hydrogen cyanide (HCN), m/z 31 formaldehyde (HCHO), m/z 33 methanol (CH_3OH), m/z 42 acetonitrile (C_2H_3CN), m/z 45 acetadehyde (C_2H_4O), m/z 47 formic acid (HCOOH), m/z 59 acetone and propanal (C_3H_6O), m/z 61 acetic acid (CH_3COOH), m/z 63 dimethyl sulphide - DMS (C_2H_6S), m/z 69 furan/isoprene (C_4H_4O/C_5H_8), m/z 71 methacrolein/methyl vinyl ketone - MVK (C_4H_6O), m/z 73 methylglyoxal ($C_3H_4O_2$)/methyl ethyl ketone - MEK

(C_4H_8O), m/z 79 benzene (C_6H_6), m/z 85 2-furanone ($C_4H_4O_2$), m/z 87 2,3-butanedione ($C_4H_6O_2$) m/z 93 toluene (C_7H_8), m/z 95 phenol (C_6H_6O), m/z 107 ethylbenzene + xylenes (C_8H_{10}), m/z 121 C_3 benzenes (C_9H_{12}), m/z 137 monoterpenes ($C_{10}H_{16}$) + unknowns ($C_8H_8O_2$). These are expected to be the dominant compounds contributing to these masses. However, due to the inability of the PTR-MS to differentiate between species with the same molecular mass, a contribution from other compounds not listed here cannot be ruled out. Protonated masses m/z 46, m/z 101, m/z 113 and m/z 153 were measured but not identified, but their concentrations have been reported in this work with the aim of quantifying as much emitted volatile carbon as possible.

During the campaign the PTR-MS was calibrated for the following compounds using certified gas standards from Scott Specialty Gases, USA and National Physical Laboratory, UK: methanol, acetaldehyde, acetone, isoprene, MVK and methacrolein, MEK, benzene, toluene, ethylbenzene, 1,2,4 trimethylbenzene and formaldehyde. Calibration data were used to construct sensitivity plots which were used to calculate approximate response factors for other masses not specifically calibrated. Due to having proton affinities similar to water, formaldehyde and HCN responses are highly dependent on humidity of the sample air. The changing response of the PTR-MS for these compounds was calculated every 10 minutes by taking the response of the dry formaldehyde calibration gas, then adjusting this based on the measured water content of the sample air and relationship between response and humidity as reported in Inomata et al (2008). Corrections were made to the response of m/z 61 and m/z 137 for known losses due to fragmentation of acetic acid and monoterpenes at those masses. Dunne et al (2012) reported a significant interference to the acetonitrile signal at m/z 42 from the ^{13}C isotopologues of $C_3H_5^+$ and the product ion $C_3H_6^+$ from reactions involving O_2^+ and alkanes/alkenes. A detailed correction for this interference was not possible here, due to an absence of m/z 41, and alkane and alkene measurements. However, during a BB event, Dunne et al., (2012) calculated a 20% contribution to m/z 42 from non-acetonitrile ions: to reflect this interference the m/z 42 signal during the BB events has been reduced by 20%. Minimum detectable limits (MDLs) were calculated according to the principles of ISO 6869 (ISO, 1995) and ranged from 2 – 563 ppt for a one hour measurement. Where measured levels were below the MDL, a half MDL value was substituted.

3 Results and discussion

A time series of CO, BC and particle number > 3nm clearly shows the two events (BB1 and BB2) where plumes from the Robbins Island fire impacted the Cape Grim Station (Fig. 2). A detailed times series of these two events are presented here, with discussion of the influence of photochemistry, meteorology and air mass back trajectory on changing composition of trace gases and aerosol.

3.1 Biomass burning event 1 (BB1) February 16th 2006

3.1.1 Brief plume strike, particle growth and ozone enhancement

Fig. 3. shows a time series plot from BB1, including both the fresh plume and the changing composition with changing wind direction. A particle size and number contour plot, wind direction, O_3, CO, BC and urban tracer HFC-134a are shown. Periods of interest are labelled asd Periods A-F (Fig 3.) which are discussed below and summarised in Table 2. Average particle size distributions for periods corresponding to Periods A-F are presented in Fig. 4. NMOC data is not available from BB1. The matching air mass back trajectories for periods corresponding to Periods A-F are shown in Supp Fig. 1a-f.

Period A. The fresh BB plume is visible from ~02:00-06:00 (Fig. 3.) through high particle number concentrations corresponding with elevated CO and BC. The BB particles have a single, broad size distribution with a dominant mode of 120 nm (Fig. 4a), indicating fresh BB aerosol (Janhäll et al., 2010). The O_3 mixing ratio during this period is 10 ppb which is lower than background concentration of about ~15 ppb, likely due to titration by NO emitted from the fire. The HYSPLIT back trajectory (Supp Fig. 1a) indicates that air which brought the plume to Cape Grim had previously passed over the north west corner of Tasmania and the Southern Ocean.

Period B. Just after 06:00 (Fig. 3.), a slight wind direction change results in dramatically reduced particle concentration, CO and BC. The dominant mode of the particles drops from about 120 nm to 50 nm, but the distribution remains broad and uni-modal (Fig. 4a). From 7:00 – 12:00 there is a gradual increase in the dominant mode of particles from 50 nm to 80 nm, which is accompanied by an increase in ozone from 12 to 20 ppb. The winds were light (1 m s^{-1}) and variable, the temperature mild (19ºC) and skies clear during this period. An increase in particle size and ozone in calm and sunny conditions suggests that particles were growing in size due to oxidation of gas phase precursors and condensation of low volatility products. An alternative but less likely explanation is that the light and variable winds were bringing increasingly larger particles and ozone to the station over several hours. There is a small enhancement of BC above background concentrations (12 - 194 ng m^{-3},) while the particle size is increasing, suggesting that the station may be on the edge of the plume during this period, however CO is not enhanced alongside BC and so influence of BB emissions cannot be confirmed. The HYSPLIT trajectory (Supp Fig. 1b) shows that air arriving at the station is almost entirely of marine origin but had some contact with the vegetated and sparsely populated North West coast of Tasmania and appears to pass over Robbins Island before arriving at Cape Grim.

Period C. At midday, the dominant particle mode stops increasing and is stable, and BC drops to background levels. An easterly wind overnight brings air from the sparsely populated and forrested coast of south eastern Australia (Supp Fig. 1 c) which leads to a further decrease in particle number, but a continued increase in O_3. The meteorology and nightime increase in O_3 is suggestive of a transported continental aged air mass arriving at Cape Grim, rather than local production. The average particle size distribution over this period (Fig. 4b) is a single broad distribution with a dominant mode of around 60nm, and is similar in shape to the distribution during the particle growth event.

Period D. A strong urban influence is visible in the early morning on the 17th February (Fig. 3.), when air is transported directly from metropolitan region of Melbourne ~300 km directly to the north (Supp Fig. 1d). O_3 peaks at ~30 ppb, accompanied by particle number concentrations of similar magnitude to the direct BB plume the previous day, but without the elevated CO or BC. The significant urban influence is confirmed by a peak in HFC-134a, an urban tracer which is widely used in motor vehicle air conditioning and domestic refrigeration (McCulloch et al., 2003). The average particle size distribution (Fig. 4b) shows a single broad distribution with a dominant mode of 90 nm.

Period E. In mid afternoon on the 17th February a westerly wind from the ocean sector leads to a sudden drop in HFC-134a, O_3 and particle number. HYSPLIT trajectories suggest the air mass passed over the ocean for at least 60 hours prior to arriving at Cape Grim (Supp Fig. 1 E). The particle size distribution changes from uni-modal to bi-modal, with dominant modes at around 50nm and 160 nm (Fig. 4c). This bi-modal distribution is typical of clean marine air and aerosols are likely dominated by non sea salt sulphate and sea salt particles, which in the larger mode have been cloud processed (Lawler et al., 2014; Cravigan et al., 2015).

Period F. At midnight on the 18th February, (Fig. 3.) terrestrial influence from mainland Australia is visible (Supp Fig. 1f), with an increase in O_3, HFC-134a and an increase in particle number in the 60 – 200nm size range. Over the next 24 hours, decreasing O_3 and particle number suggests the air is becoming increasingly free of terrestrial influence. However the HYSPLIT trajectory (Supp 1F) shows that some terrestrial influence from mainland Australia remains for the next 24 hours. This is also shown by HFC-134a values which are slightly higher than during clean marine period (Event E), and a uni-model average particle size distribution (Fig. 4c), which resembles the terrestrially-influenced distributions corresponding to Periods B, C, D and F.

It is interesting to note that while size distributions have been described as uni-modal for Periods B, C, D and F, Fig. 4 a-c shows evidence of a second minor mode at around 160-170 nm in each of these terrestrially-influenced periods. Due to the strong marine influence of the air arriving at Cape Grim, the 160-170 nm mode in these periods can likely be attributed to cloud processed non sea salt sulphate and sea salt aerosol, and corresponds to the second larger mode (160 nm) in the clean marine period of Fig. 3 Period E.

Of interest is the contribution that the BB emissions from the Robbins Island fire had on the O_3 enhancement (Fig. 3). Determining the contribution is challenging given the variety of emission sources impacting Cape Grim (BB, terrestrial, marine, urban), and understanding the transport and mixing of these emissions. During BB1 The HFC-134a indicates an increasing influence from urban air from mainland Australia (indicating a likely source of O_3 or O_3 precursors), and indeed the O_3 and HFC-134a concentrations do increase in parallel (Fig. 3). However, some of the increases in O_3 occured when there was minimal urban influence, for example during the particle growth event (Fig. 3 Period B), and may have been driven by emissions from the local fire. Use of a chemical transport model to determine influence of fire emissions on O_3 formation will be reported in a follow up paper by Lawson et al (2015).

3.1.2 Ability of particles in BB event 1 (BB1) to act as CCN

The ability of particles to act as CCN at 0.5% supersaturation was investigated during the fresh BB plume (Fig. 3 Period A) and the particle growth period (Period B). The CCN activity of particles was also calculated during the 24 hours of Period F, chosen due to the absence of BB tracers during this period, and predominance of marine air with some minor terrestrial influence. The average hourly ratio of CCN number to condensation nuclei (CN) number > 80 nm (CN80, measured using the SMPS) was calculated. CN80 was chosen based on a study by Petters et al., (2009) which suggested even weakly hygroscopic BB aerosols began to activate to CCN at a diameter of approximately 80 nm and larger. Given this, any observed difference in the CCN/CN80 ratio may then be due to either different chemical composition between the particles, and/or differences in particles size distributions, as larger particles are more easily activated to CCN. The CCN/CN80 ratio has only been calculated for BB1 because there are no aerosol size distribution measurements (and hence no CN80 measurements) for BB2.

Fig. 5a shows the CCN/CN80 expressed as a percentage for the fresh plume (Period A), particle growth event (Period B), and background marine/terrestrial (Period F). Error bars are ±1 standard error of the mean. Fig. 5b shows the absolute number concentration of CCN during these periods.

The CCN/CN80 ratio during the fresh BB plume strike (Period A) is 56±8%. Petters et al., (2009) show that in laboratory BB measurements the CCN activation of 80 nm particles ranges from a few % for low or weakly hygroscopic fuels to up to 60% for more hygroscopic fuels such as chamise, suggesting that the particles produced from coastal heath burned here may be more hygroscopic than those from other fuel types.

The CCN/CN80 ratio is substantially higher during the particle growth event (Period B) (77±4%). Fig. 4a shows that the average dominant diameter of particles shifts from around 120 nm during Period A to around 60nm during Period B. The smaller diameter during Period B suggests that particle size is not the reason for the increased CCN/CN80 ratio during the particle growth period, but is likely due to a changing chemical composition of particles between the two periods, with more hygroscopic particles measured during the particle growth period compared to the fresh BB particles. Volatility and hygroscopicity measurements of particles are available from Period A using a volatility and hygroscopic tandem differential mobility analysis (VH-TDMA) system (Fletcher et al., 2007). These measurements focused on the composition of 60 nm particles, and suggested they consisted of a non-hygroscopic 23-nm core, a hygroscopic layer to 50 nm and a hydrophobic outer layer to 60 nm (possible homogeneously mixed). There was some evidence that the particle core contained two different types of particle, possibly due to merging of marine and BB particles. The suggested mix of hygroscopic and non-hygroscopic materials in fresh BB particles is in agreement with the fact that only 56% of these particles were hygroscopic enough to act as CCN. While the composition of the fresh BB particles may only be inferred from these measurements, the non-hygroscopic core may be black carbon or primary organic aerosol, the hygroscopic component an inorganic material such as sea salt or ammonium nitrate or sulphate or a hydroscopic organic such as MSA which is abundant in the marine boundary layer at Cape Grim in summer. The hydrophobic outer layer may be a hydrocarbon-type organic, with a low O:C ratio, which was co-emitted in the fire and condensed on to the particle as the plume cooled and was transported to Cape Grim (Fletcher et al., 2007). Unfortunately no hygroscopicity or volatility measurements are available from Period B (particle growth).

During background marine Period F, all (104 ± 3%) of the particles >80 nm could act as CCN (Fig. 5a). A value of more than 100% is not physically possible but is due to uncertainty associated with the different techniques (SMPS and CCN) and measurement synchronisation. This result is in agreement with the work of Fletcher et al (2007) who reported that the fresh BB particles from BB1-A had a lower hygroscopic growth factor than marine particles. Fig. 4 a and 4 c shows the average size distribution of particles during Period F (background marine/terrestrial) is very similar to period B (particle growth), despite the air masses coming from different directions (westerly and easterly respectively). As discussed previously, both these periods have a predominent marine back trajectory and some terrestrial influence. It is therefore likely that the main difference between the particle composition between these two periods, and the reason for the lower CCN/CN ratio during Period B is the presence of non or weakly-hygroscopic >80 nm particles, such as the BC which elevated above background levels during Period B.

Sea salt and non sea salt sulphate aerosol are important sources of CCN in the marine boundary layer (Korhonen et al., 2008; Quinn and Bates, 2011) and are likely the main source of CCN in Period F (and possibly Period B). The fact that all particles >80nm could act as CCN in Period F suggests that any non-hygroscopic terrestrial particles which reached Cape Grim during this time were likely to have been aged and oxidised during the several hundred kms during transport from the mainland.

Finally, the absolute number concentration of CCN in the fresh plume (A) (hourly average) was ~2000 cm^{-3} (Fig. 5b), with minute average concentrations up to ~5500 CCN cm^{-3}. In contrast, the average number of CCN during particle growth (Period B) was a factor of 3 lower at ~700 CCN cm^{-3}. During the background marine/terrestrial Period (F) in BB1, the CCN is 320 CCN cm^{-3}, with low variability, a value which is within the range of typical pristine marine values (Gras, 2007). Overall, CCN were enhanced by a factor ~6 and a factor of ~30 above background levels in BB1 and BB2 respectively (see Sect. 3.2 and Table 3). Despite the modest ability of fresh BB particles to form CCN (CCN/CN80 ratio of 56%), the very high numbers of particles ejected into the marine boundary layer during the fire highlights the dramatic impact BB plumes can have on the CCN population, particularly in clean marine regions.

3.2 BB event 2 (BB2) February 23rd 2006

3.2.1 Interplay between emissions, meteorology and sources

BB2 was of much longer duration than BB1, and lasted about 29 hours. Fig. 6 shows a time series including wind direction and rainfall, O_3, CO, BC, BB tracer acetonitrile, acetonitrile/CO ratio (where CO > 400 ppb) and urban tracer HFC-134a. Periods of interest are highlighted as A-D (Fig 6.), summarised in Table 2 and discussed below. Particle size distribution data is not available for BB2. The matching air mass back trajectories for the events highlighted in Fig. 6. are shown in Supplementary Fig. 2. a-d.

Period A. For the first 24 hours of BB2, there is clear elevation in CO, BC and acetonitrile, due to the easterly wind advecting the plume directly to Cape Grim. The acetonitrile mixing ratio is ~ 1 ppb and is enhanced by a factor of 30 above typical background levels at Cape Grim of ~35 ppt (Table 3). The acetonitrile ratio to CO is also relatively constant during this time (1-2 ppt/ppb). An ozone peak of 27 ppb (minute data) occurs in mid afternoon on 24 February, corresponding to an hourly Normalised Excess Mixing Ratio (NEMR) $\Delta O_3/\Delta CO$ of 0.05 (where NEMR is an excess mixing ratio normalised to a non-reactive co-emitted tracer, in this case CO, see Akagi et al., 2011).

Period B. At 04:00 on 25th February acetonitrile peaks by a factor of 17 over 2 hours (Fig. 6 Period B) with a smaller peak at 23:00 on the 24th February. Almost all masses on the PTR-MS increased at the same time as acetonitrile, including masses corresponding to HCN, methanol, acetaldehyde, acetone, furan/isoprene and benzene). The corresponding CO peak at 04:00 (~1500 ppb) increased by a factor of 21 and is the largest peak from BB2. The corresponding BC peak at 04:00 is much smaller than peaks which occured earlier in BB2. This large enhancement in CO and NMOCs but modest enhancement in BC suggests a decrease in the combustion efficiency during this time. This is further supported by increases in the ratio of acetonitrile to CO (where CO > 400 ppb) by a factor of ~3 during the peak periods (Fig. 6), and a decrease in the ratios of BC to CO during peak periods (average 0.9± 0.3 ng $m^{-3}ppb^{-1}$) compared to non-peak periods (2.2± 0.1 ng $m^{-3}ppb^{-1}$).

A small amount of rainfall recorded at Cape Grim (1.4 mm) corresponds with the second peak (Fig. 6). Archived radar images from the Bureau of Meteorology (West Takone 128 km, 10 min resolution) confirm that very light patchy rain showers occured on Robbins Island at 23:10 followed by intermittent rain showers of light to moderate intensity from 12:40 until 05:40, on the 25th February (S. Baly, pers com). The total rainfal amount that fell on Robbins Island was between 1-5 mm (www.bom.gov.au). Evidence of rainfall coinciding with an enhancement in NMOC ER to CO, and a decrease in BC ER to CO suggests that the rainfall changed the combustion processes of the fire. The enhanced ERs of NMOCs to CO which are associated with low-efficiency, smouldering combustion, can therefore attributed to a short term decrease in combustion efficiency, driven by rainfall. Due to the small number of data points (2) it is not possible to calculate reliable ER to CO during this shortlived event. But this time series highlights the importance of relatively minor meterological events on BB emission ratios.

While the elevated concentrations of BB tracers CO, BC and acetonitrile during this period are attributed to emissions from the local fire, back trajectories (Supp Fig. 3B) show that air arriving at Cape Grim had previously passed over the Australian mainland. The increasing anthropogenic influence is also supported by increasing levels of HFC-134a and a corresponding increase in O_3 which peaks at 34 ppb (minute data) at 1:00-2:00, with an hourly NEMR for $\Delta O_3/\Delta CO$ of 0.07 (the highest observed).

Period C. With a change in wind direction further to the north from 5:00 onwards (Fig. 6), BB tracers BC, CO and acetonitrile all decrease to background levels, indicating fire emissions are no longer impacting the station. Ozone begins to increase at 8:00 and reaches ~40 ppb 3 hours later, corresponding with a maximum HFC-134a mixing ratio of ~ 35 ppt. The air mass back trajectory (Supp Fig. 2 C) confirms that air from Melbourne is impacting the station during this period

Period D. As wind moves further into the west in to the clean marine sector (Supp Fig. 2D), O_3 and HFC-134a decrease to background levels.

This time series highlights possible interplay of sources and meteorology on the observed trace gases and particles. The very large increase of NMOCs and CO observed during the rainfall period shows the potentially large affect of quite minor meteorological events on BB emission ratios. While other studies have found a link between fuel moisture, MCE and emissions of PM2.5, (eg Watson et al., 2011 ; Hosseini et al., 2013) this is the first study to our knowledge which has linked rainfall with a large increase in trace gas emission ratios from BB.

This work also highlights the large influence that BB plumes can have on the composition of air in the marine boundary layer. During the direct plume strikes, absolute numbers of particles > 3nm increased from 600 to 25,000 particles cm^{-3} (hourly average). In BB2, as was the case in BB1, the O_3 concentrations closely correspond with the HFC134a concentrations. This suggests that transport of photochemically processed air from urban areas to Cape Grim is the main driver of the O_3 observed but does not rule out possible local O_3 formation from BB emissions. NEMRs of $\Delta O_3/\Delta CO$ ranged from 0.001-0.074 during BB2 which are comparable to NEMRs observed elsewhere in BB plumes <1 hr old (Yokelson et al., 2003;Yokelson et al., 2009).

3.2.2 Chemical composition of BB2 and selection of in-plume and background periods

The composition of the fresh plume during BB2 was explored by determining for which trace gas and aerosol species the enhancement above background concentrations was statistically significant. Emission ratios (ER) and particle number to CO were then calculated for these selected species and converted to emission factors (EF).

The first 10 hours of Period A from BB2 (from 23:00 on the 23rd Feb to 09:00 on the 24th Feb) was selected to characterise the fresh plume composition. During this time, the air which brought the Robbins Island BB emissions to Cape Grim had previously passed over the ocean and so was free of terrestrial or urban influence (NOAA HYSPLIT Supp Fig. 2A). While fresh BB emissions were measured at Cape Grim beyond 10:00 on the 24th Feb, the air at this time had prior contact with the Australian mainland, including the Melbourne region and so was considered unsuitable for characterising the BB plume. During the selected time period, wind speeds of 16 m s^{-1} meant that the plume travelled the 20 km to Cape Grim over a period of about 20 minutes, which allows the plume to cool to ambient temperatures but ensured minimum photochemical processing of the plume (Akagi et al., 2011). Advection of the plume to the site occurred primarily at night so minimal impact of photochemical reactions on the plume composition is expected (Vakkari et al., 2014). It is therefore assumed that the enhancement ratios measured at Cape Grim during this time are unaltered from the original emission ratios. Finally, photos indicate the Robbins Island fire plume was well mixed within the boundary layer and was not lofted into the FT, allowing representative ‘fire-averaged’ measurements to be collected (Akagi et al., 2014).

Background concentrations of gas and particle species were determined from fire-free periods in early March 2006 which had a very similar air back trajectory to trajectories during the fire (not shown). Concentrations of long lived urban tracers (not emitted from fires) including HFC-32, HFC-125a and HFC-134a were also used to match suitable background time periods with the fresh plume period.

Table 3 lists the gas and aerosol species measured, whether concentrations were statistically higher in the plume compared to background air, average background concentrations, average in-plume concentrations, emission ratios (ER) to CO and EF (g kg^{-1}). Details of ER and EF calculations are given below. Hourly average data were used for these calculations.

3.2.3 Species emitted in BB event 2 (BB2) –t tests

Hypothesis testing using the student t tests (one sided) were carried out to determine whether concentrations in the BB plume (x_1) were significantly higher than concentrations observed in the background periods (x_2), with a 95% level of significance. Table 3 shows which species were statistically enhanced in the BB plume, and hence assumed to be emitted from the fire (x_1-x_2>0) and those which were not statistically enhanced in the BB plume (x1-x2=0). While the vast majority of species measured were found to be significantly enhanced in the BB plume, there were a number of species including DMS, chloroform, methyl chloroform, dichloromethane, carbon tetrachloride, bromoform and the urban tracers HFC-032, HFC-125 and HFC-134a which were not significantly enhanced. DMS has consistently been found to be emitted from BB in many studies (as summarised by Akagi et al 2011). However, in this study due to close proximity to the ocean, the likely emission of DMS from the BB was likely obscured by the high variability in the background concentration. The absence of emission of chloroform, methyl chloroform, dichloromethane, carbon tetrachloride, tribromomethane and the HFCs are in agreement with a recent study of boreal forest emissions by Simpson et al (2011).

3.2.4 Calculation of Emission Ratios to CO

Excess mixing ratios (Δx) were calculated for species that were statistically higher in the plume compared to background air by subtracting background mixing ratios from the hourly in-plume mixing ratios. Emission ratios to CO were then calculated by plotting Δx versus ΔCO, fitting a least squares line to the slope and forcing the intercept to zero (Yokelson et al., 1999). Emission ratios (ER) to CO and the R^2 of the fit are reported in Table 3.

The excess mixing ratios of all species significantly enhanced in the plume correlated with the excess mixing ratios of CO with an R^2 value of ≥ 0.4, with the exception of CO_2, HCHO, HCOOH, m/z 101, N_2O, and CCN number concentration (see discussion below and Fig. 3b). ER plots for BC, CN>3nm, H_2, CH_4, C_2H_6, C_6H_6, CH_3COOH, C_6H_6O and C_2H_3N are shown in Fig. 7. The ER of CO to particle number (38 cm^{-3} ppb^{-1}) agrees well with a literature averaged value of 34 ± 16 cm^{-3} ppb^{-1} (Janhall., et al 2010). The H_2 ER to CO (0.10) is lower than the range reported from BB emissions (0.15-0.45), as summarised by Vollmer et al., (2012).

There is a low correlation between mixing ratios of CO and CO_2 (ER to CO R^2 = 0.15, see Table 3). This is in part because CO and CO_2 are emitted in different ratios from different combustion processes (smouldering and flaming respectively) and may also be influence by variability in background levels of CO_2 (Andreae et al., 2012). Of the other species with R^2 values of <0.4, HCHO and HCOOH are both emitted directly from BB, but are also oxidation products of other species co-emitted in BB. It is therefore possible that in the 20 minute period between plume generation and sampling, chemical processing has lead to generation of these compounds in the plume, which has changed the ER to CO. In addition, sampling losses of HCOOH down the inlet line are possible (Stockwell et al., 2014). The lack of relationship between ΔCO and ΔN_2O is likely because N_2O is an intermediate oxidation product which is both formed and destroyed during combustion. Studies of emissions from Savanna burning in Northern Australia have found N_2O to be insensitive to changes in MCE (Meyer and Cook, 2015; Meyer et al., 2012; Volkova et al., 2014). A further reason for a lack of correlation with ΔCO for ΔN_2O is that as for CO_2, the plume enhancement of ΔN_2O is relatively small compared to the observed variability in background concentrations. Finally the lack of correlation between ΔCCN and ΔCO may be due interaction of plume aerosol with background sources of CCN, such as sea salt, and the change in particle properties and composition in the 20 minutes after emission.

3.2.5 Calculation of MCE and EF and comparison with other studies

Combustion efficiency (CE) is a commonly used measure of the degree of oxidation of fuel carbon to CO_2. Combustion efficiency is commonly approximated as the modified combustion efficiency (MCE) (Yokelson et al., 1999), which is calculated using the following equation

$$MCE = \frac{\Delta CO_2}{\Delta CO_2 + \Delta CO} \qquad (1)$$

In this study the 10 hour integrated MCE was 0.88, which indicates predominantly smouldering combustion. The ER of BC to CO reported here is in good agreement with BC to CO ERs in smouldering fires (MCE <0.9) reported by Kondo et al., (2011) and May et al., (2014) which suggests that the excess CO_2, and MCE has been determined reliably.

Whole of fire Emission factors were calculated according to the Carbon Mass Balance method (Ward and Radke, 1993). Emission factors were calculated relative to combusted fuel mass (Andreae and Merlet, 2001), assuming 50% fuel carbon content by dry weight according to the following equation.

$$EFx(g/kg) = \frac{[\Delta x]}{\sum([\Delta CO_2] + [\Delta CO] + [\Delta CH_4])} \times 0.5 \times 1000(g/kg) \times \frac{MW(x)}{12} \qquad (2)$$

The Carbon Mass Balance method assumes all volatilised carbon is detected, including CO_2, CO, hydrocarbons and particulate carbon. Here the major volatile carbon components of CO_2, CO and CH_4 were used in the EF calculation, so the resulting EF may be overestimated by 1-2 % (Andreae and Merlet, 2001).

For comparison with the carbon mass balance method, EF were also calculated using an average CO EF for temperate forests from Akagi et al (2011), which corresponds to an MCE of 0.92 (see Supplementary material for EF and method details). Trace gas EF calculated using an assumed CO EF were generally 50% lower than EF calculated using the carbon mass balance method.

Table 4 shows EFs calculated from this study (Carbon Mass Balance Method) compared with other Australian BB studies both of eucalypt and schlerophyll forest fires in temperate south eastern Australia (Paton-Walsh et al., 2005; Paton-Walsh et al., 2008; Paton-Walsh et al., 2014), and tropical savanna fires in northern Australia (Paton-Walsh et al., 2010; Meyer et al., 2012; Hurst et al., 1994a; Hurst et al., 1994b; Shirai et al., 2003; Smith et al., 2014). The fire in this study (41ºS) is >1000 km south of the temperate forest fires used for comparison (33-35ºS), and some 2500 km South East of the tropical savannah fires in the comparison (12-14ºS).

EF from this study reported in Table 4 are within 50% of the EFs from the other South Eastern Australian studies except for acetic acid, which is 5 times lower than the EF reported by Paton-Walsh et al., (2014). EF from this study are also within 50% of temperate NH EF (temperate forests and chaparral) except for hydrogen, acetic acid and the methyl halides and within 80% of the average tropical savannah EF, with the exception of acetic acid and the methyl halides.

The acetic acid EF from this study is significantly lower than reported from Australian and NH temperate studies, though the variability reported elsewhere is large. Acetic acid may form rapidly in BB plumes (Akagi et al., 2012), which adds uncertainty to the EF in plumes which are sampled some distance downwind of emission. The lower EF reported in this work may be due to inlet losses, or another loss process such as nocturnal uptake of acetic acid on to wet aerosols (Stockwell et al., 2014).

The methyl halides EF from this study are in the same proportion as seen elsewhere (i.e. EF (CH_3Cl) > EF(CH_3Br) > EF(CH_3I) but the EF magnitudes are substantially higher. The CH_3Cl EF from this study is more than a factor of 4 higher than elsewhere in Australia and the NH, the CH_3Br EF between 5 and 11 times higher and CH_3I EF a factor of about 3 times higher than elsewhere. EF calculated by the alternative ER to CO method (Supplementary material) gives methyl halide EFs which are 30% lower but still much larger than those observed elsewhere. It is likely that the high methyl halide EFs reported here are due to high halogen content of soil and vegetation on the island, due to very close proximity to the ocean, and transfer of halogens to the soil via sea spray (McKenzie et al., 1996). Chlorine and bromine content in vegetation has been shown to increase with proximity to the coast (McKenzie et al., 1996; Stockwell et al., 2014) and methyl chloride and hydrochloric acid EF are impacted by the chlorine content of vegetation (Reinhardt and Ward, 1995; Stockwell et al., 2014).

4 Summary and future work

The opportunistic measurement of BB plumes at Cape Grim Baseline Air Pollution Station in February 2006 has allowed characterisation of BB plumes in a region with few BB measurements. Plumes were measured on two occasions (events BB1 and BB2) when the plume was advected to Cape Grim from a fire on Robbins Island some 20 km to the east.

The fresh plume had a large impact on the number of particles at Cape Grim, with absolute numbers of particles > 3 nm increasing from 600 cm^{-3} in background air up to 25,000 cm^{-3} during the fresh plume in BB2 (hourly average) and CCN increasing from 160 cm^{-3} in background air up to 5500 cm^{-3} (hourly average). The dominant particle diameter mode measured in BB1 was 120 nm.

After a slight wind direction change, BB tracers BC and CO decreased dramatically and the dominant particle mode decreased to 50nm. A gradual increase in particle size to 80nm was observed over 5 hours, in calm sunny conditions, alongside a modest increase in ozone. BC was present above background levels during particle growth but CO was not significantly elevated, so the presence of the fire emissions during particle growth cannot be determined. . During BB1, the ability of particles > 80nm to act as CCN at 0.5% supersaturation was investigated, including during the fresh BB, particle growth and background terrestrial/marine periods. The ΔCCN/ΔCN80 ratio was lowest during the fresh BB plume strike (56±8%), higher during the particle growth event (77±4%) and is higher still (104±3%) in background marine air.

Enhancements in O_3 concentration above background were observed following the direct plume strikes in BB1 and during the direct plume strike in BB2, with NEMRs ($\Delta O_3/\Delta CO$) of 0.001-0.074. It is likely that some of the O_3 enhancement that occured during the particle growth event in BB1 was driven by fire emissions. However on other occasions enhancement of O_3 which occured at night, corresponding with enhancements of urban tracer HFC-134a was most likely due to air being transported from mainland Australia. Chemical transport modelling will be used in a follow up paper to elucidate the sources, and where possible the species responsible for the O_3 enhancement and change in particle hygroscopicity observed, as well as the age of the urban emissions transported from Melbourne.

The more prolonged BB2 allowed determination of emission ratios (ER) to CO and Emission Factors (EF) for a range of trace gas species, CN and BC using the carbon mass balance method. These EF, which were calculated from nocturnal measurements of the BB plume, provide a unique set of emission estimates for a wide range of trace gases from burning of coastal heathland in temperate Australia.

A very large increase in emissions of NMOCs (factor of 16) and CO (factor of 21), and a more modest increase in BC (factor of 5) occurred during BB2. The ratio of acetonitrile to CO increased by a factor of 2-3 and the ratio of BC to CO halved during this period. This change in emission ratios is attributed to decreased combustion efficiency during this time, due to rainfall over Robbins Island. Given that air quality and climate models typically use a fixed EF for trace gas and aerosol species, the impact of varying emissions due to meteorology may not be captured by models.

More broadly, given the high variability in reported EF for trace gas and aerosol species in the literature, the impact of EF variability on modelled outputs of both primary BB species (i.e. CO, BC, NMOCs) and secondary BB species (i.e. O_3, oxygenated NMOCs, secondary aerosol) is likely to be significant. In the next phase of this work, in addition to exploring the chemistry described above with chemical transport modelling, we will also systematically explore the sensitivity of these models to EF variability, as well as spatial and meteorological variability.

Acknowledgements

The Cape Grim program, established by the Australian Government to monitor and study global atmospheric composition, is a joint responsibility of the Bureau of Meteorology (BOM) and the Commonwealth Scientific and Industrial Research Organisation (CSIRO). We thank the staff at Cape Grim and staff at CSIRO Oceans and Atmosphere (Rob Gillett, Suzie Molloy) for their assistance and input. We acknowledge the NOAA Air Resources Laboratory (ARL) for the provision of the HYSPLIT transport and dispersion model used in this publication. West Takone radar images courtesy of Stuart Baly (BOM). We thank both reviewers for insightful comments and suggestions which have been incorporated into the manuscript.

References

Akagi, S. K., Yokelson, R. J., Wiedinmyer, C., Alvarado, M. J., Reid, J. S., Karl, T., Crounse, J. D., and Wennberg, P. O.: Emission factors for open and domestic biomass burning for use in atmospheric models, Atmospheric Chemistry and Physics, 11, 4039-4072, 10.5194/acp-11-4039-2011, 2011.

Akagi, S. K., Craven, J. S., Taylor, J. W., McMeeking, G. R., Yokelson, R. J., Burling, I. R., Urbanski, S. P., Wold, C. E., Seinfeld, J. H., Coe, H., Alvarado, M. J., and Weise, D. R.: Evolution of trace gases and particles emitted by a chaparral fire in California, Atmospheric Chemistry and Physics, 12, 1397-1421, 10.5194/acp-12-1397-2012, 2012.

Akagi, S. K., Yokelson, R. J., Burling, I. R., Meinardi, S., Simpson, I., Blake, D. R., McMeeking, G. R., Sullivan, A., Lee, T., Kreidenweis, S., Urbanski, S., Reardon, J., Griffith, D. W. T., Johnson, T. J., and Weise, D. R.: Measurements of reactive trace gases and variable O3 formation rates in some South Carolina biomass burning plumes, Atmos. Chem. Phys., 13, 1141-1165, 10.5194/acp-13-1141-2013, 2013.

Akagi, S. K., Burling, I. R., Mendoza, A., Johnson, T. J., Cameron, M., Griffith, D. W. T., Paton-Walsh, C., Weise, D. R., Reardon, J., and Yokelson, R. J.: Field measurements of trace gases emitted by prescribed fires in southeastern US pine forests using an open-path FTIR system, Atmospheric Chemistry and Physics, 14, 199-215, 10.5194/acp-14-199-2014, 2014.

Alvarado, M. J., Lonsdale, C. R., Yokelson, R. J., Akagi, S. K., Coe, H., Craven, J. S., Fischer, E. V., McMeeking, G. R., Seinfeld, J. H., Soni, T., Taylor, J. W., Weise, D. R., and Wold, C. E.: Investigating the links between ozone and organic aerosol chemistry in a biomass burning plume from a prescribed fire in California chaparral, Atmos. Chem. Phys., 15, 6667-6688, 10.5194/acp-15-6667-2015, 2015.

Andreae, M. O., and Merlet, P.: Emission of trace gases and aerosols from biomass burning, Global Biogeochemical Cycles, 15, 955-966, 10.1029/2000gb001382, 2001.

Andreae, M. O., Artaxo, P., Brandao, C., Carswell, F. E., Ciccioli, P., da Costa, A. L., Culf, A. D., Esteves, J. L., Gash, J. H. C., Grace, J., Kabat, P., Lelieveld, J., Malhi, Y., Manzi, A. O., Meixner, F. X., Nobre, A. D., Nobre, C., Ruivo, M., Silva-Dias, M. A., Stefani, P., Valentini, R., von Jouanne, J., and Waterloo, M. J.: Biogeochemical cycling of carbon, water, energy, trace gases, and aerosols in Amazonia: The LBA-EUSTACH experiments, Journal of Geophysical Research-Atmospheres, 107, 8066, 10.1029/2001jd000524, 2002.

Andreae, M. O., Artaxo, P., Beck, V., Bela, M., Freitas, S., Gerbig, C., Longo, K., Munger, J. W., Wiedemann, K. T., and Wofsy, S. C.: Carbon monoxide and related trace gases and aerosols over the Amazon Basin during the wet and dry seasons, Atmospheric Chemistry and Physics, 12, 6041-6065, 10.5194/acp-12-6041-2012, 2012.

Buckby, P.: Robbins Island Saga, The Commercial Finance Company of Tasmania Pty Ltd, Smithton Tasmania, 1988.

Cainey, J. M., Keywood, M., Grose, M. R., Krummel, P., Galbally, I. E., Johnston, P., Gillett, R. W., Meyer, M., Fraser, P., Steele, P., Harvey, M., Kreher, K., Stein, T., Ibrahim, O., Ristovski, Z. D., Johnson, G., Fletcher, C. A., Bigg, E. K., and Gras, J. L.: Precursors to Particles (P2P) at Cape Grim 2006: campaign overview, Environmental Chemistry, 4, 143-150, 10.1071/en07041, 2007.

Christian, T. J., Kleiss, B., Yokelson, R. J., Holzinger, R., Crutzen, P. J., Hao, W. M., Saharjo, B. H., and Ward, D. E.: Comprehensive laboratory measurements of biomass-burning emissions: 1. Emissions from Indonesian, African, and other fuels, Journal of Geophysical Research-Atmospheres, 108, 10.1029/2003jd003704, 2003.

Christian, T. J., Kleiss, B., Yokelson, R. J., Holzinger, R., Crutzen, P. J., Hao, W. M., Shirai, T., and Blake, D. R.: Comprehensive laboratory measurements of biomass-burning emissions: 2. First intercomparison of open-path FTIR, PTR-MS, and GC- MS/FID/ECD, Journal of Geophysical Research-Atmospheres, 109, 12, D02311

10.1029/2003jd003874, 2004.

Cravigan, L. T., Ristovski, Z., Modini, R. L., Keywood, M. D., and Gras, J. L.: Observation of sea salt fraction in sub-100 nm diameter particles at Cape Grim, Journal of Geophysical Research: Atmospheres, 2014JD022601, 10.1002/2014JD022601, 2015.

Cubison, M. J., Ortega, A. M., Hayes, P. L., Farmer, D. K., Day, D., Lechner, M. J., Brune, W. H., Apel, E., Diskin, G. S., Fisher, J. A., Fuelberg, H. E., Hecobian, A., Knapp, D. J., Mikoviny, T., Riemer, D., Sachse, G. W., Sessions, W., Weber, R. J., Weinheimer, A. J., Wisthaler, A., and Jimenez, J. L.: Effects of aging on organic aerosol from open biomass burning smoke in aircraft and laboratory studies, Atmospheric Chemistry and Physics, 11, 12049-12064, 10.5194/acp-11-12049-2011, 2011.

de Gouw, J., and Warneke, C.: Measurements of volatile organic compounds in the earths atmosphere using proton-transfer-reaction mass spectrometry, Mass Spectrometry Reviews, 26, 223-257, 10.1002/mas.20119, 2007.

Dunne, E., Galbally, I. E., Lawson, S. J., and Patti, A.: Interference in the PTR-MS measurement of acetonitrile at *m*/*z* 42 in polluted urban air—A study using switchable reagent ion PTR-MS, International Journal of Mass Spectrometry, In press, 10.1016/j.ijms.2012.05.004, 2012.

Engelhart, G. J., Hennigan, C. J., Miracolo, M. A., Robinson, A. L., and Pandis, S. N.: Cloud condensation nuclei activity of fresh primary and aged biomass burning aerosol, Atmospheric Chemistry and Physics, 12, 7285-7293, 10.5194/acp-12-7285-2012, 2012.

Ferek, R. J., Reid, J. S., Hobbs, P. V., Blake, D. R., and Liousse, C.: Emission factors of hydrocarbons, halocarbons, trace gases and particles from biomass burning in Brazil, Journal of Geophysical Research: Atmospheres, 103, 32107-32118, 10.1029/98JD00692, 1998.

Fletcher, C. A., Johnson, G. R., Ristovski, Z. D., and Harvey, M.: Hygroscopic and volatile properties of marine aerosol observed at Cape Grim during the P2P campaign, Environmental Chemistry, 4, 162-171, 10.1071/en07011, 2007.

Galbally, I. E., Lawson, S. J., Weeks, I. A., Bentley, S. T., Gillett, R. W., Meyer, M., and Goldstein, A. H.: Volatile organic compounds in marine air at Cape Grim, Australia, Environmental Chemistry, 4, 178-182, 10.1071/en07024, 2007.

Galbally, I. E., Meyer, C. P., Bentley, S. T., Lawson, S. J., and Baly, S. B.: Reactive gases in near surface air at Cape Grim, 2005-2006 Baseline Atmospheric Program (Australia), edited by: Cainey, J.M., Derek, N. and Krummel, P.B., Australian Bureau of Meteorology and CSIRO Marine and Atmospheric Research, 77-79, 2007b, available at: http://www.bom.gov.au/inside/cgbaps/baseline/Baseline_2005-2006.pdf

Gras, J. L.: Particles Program Report, 2005-2006 Baseline Atmospheric Program (Australia), edited by: Cainey, J.M., Derek, N. and Krummel, P.B., Australian Bureau of Meteorology and CSIRO Marine and Atmospheric Research, 85-86, 2007, available at: http://www.bom.gov.au/inside/cgbaps/baseline/Baseline_2005-2006.pdf

Hecobian, A., Liu, Z., Hennigan, C. J., Huey, L. G., Jimenez, J. L., Cubison, M. J., Vay, S., Diskin, G. S., Sachse, G. W., Wisthaler, A., Mikoviny, T., Weinheimer, A. J., Liao, J., Knapp, D. J., Wennberg, P. O., Kurten, A., Crounse, J. D., St Clair, J., Wang, Y., and Weber, R. J.: Comparison of chemical characteristics of 495 biomass burning plumes intercepted by the NASA DC-8 aircraft during the ARCTAS/CARB-2008 field campaign, Atmospheric Chemistry and Physics, 11, 13325-13337, 10.5194/acp-11-13325-2011, 2012.

Hennigan, C. J., Miracolo, M. A., Engelhart, G. J., May, A. A., Presto, A. A., Lee, T., Sullivan, A. P., McMeeking, G. R., Coe, H., Wold, C. E., Hao, W. M., Gilman, J. B., Kuster, W. C., de Gouw, J., Schichtel, B. A., Collett, J. L., Kreidenweis, S. M., and Robinson, A. L.: Chemical and physical transformations of organic aerosol from the photo-oxidation of open biomass burning emissions in an environmental chamber, Atmospheric Chemistry and Physics, 11, 7669-7686, 10.5194/acp-11-7669-2011, 2011.

Hennigan, C. J., Westervelt, D. M., Riipinen, I., Engelhart, G. J., Lee, T., Collett, J. L., Pandis, S. N., Adams, P. J., and Robinson, A. L.: New particle formation and growth in biomass burning plumes: An important source of cloud condensation nuclei, Geophysical Research Letters, 39, L09805, 10.1029/2012gl050930, 2012.

Hosseini, S., Urbanski, S. P., Dixit, P., Qi, L., Burling, I. R., Yokelson, R. J., Johnson, T. J., Shrivastava, M., Jung, H. S., Weise, D. R., Miller, J. W., and Cocker, D. R.: Laboratory characterization of PM emissions from combustion of wildland biomass fuels, Journal of Geophysical Research-Atmospheres, 118, 9914-9929, 10.1002/jgrd.50481, 2013.

Hurst, D. F., Griffith, D. W. T., Carras, J. N., Williams, D. J., and Fraser, P. J.: Measurements of trace gases emitted by australian savanna fires during the 1990 dry season, Journal of Atmospheric Chemistry, 18, 33-56, 10.1007/bf00694373, 1994a.

Hurst, D. F., Griffith, D. W. T., and Cook, G. D.: Trace gas emissions from biomass burning in tropical australian savannas, Journal of Geophysical Research-Atmospheres, 99, 16441-16456, 10.1029/94jd00670, 1994b.

ISO: ISO 6879 Air Quality, Performance Characteristics and Related Concepts for Air Quality Measuring Methods, in, ISO, Geneva, 1995.

Inomata, S., Tanimoto, H., Kameyama, S., Tsunogai, U., Irie, H., Kanaya, Y., and Wang, Z.: Technical Note: Determination of formaldehyde mixing ratios in air with PTR-MS: laboratory experiments and field measurements, Atmospheric Chemistry and Physics, 8, 273-284, 2008.

Jaffe, D. A., and Wigder, N. L.: Ozone production from wildfires: A critical review, Atmospheric Environment, 51, 1-10, 10.1016/j.atmosenv.2011.11.063, 2012.

Janhäll, S., Andreae, M. O., and Pöschl, U.: Biomass burning aerosol emissions from vegetation fires: particle number and mass emission factors and size distributions, Atmos. Chem. Phys., 10, 1427-1439, 10.5194/acp-10-1427-2010, 2010.

Karl, M., Gross, A., Leck, C., and Pirjola, L.: Intercomparison of dimethylsulfide oxidation mechanisms for the marine boundary layer: Gaseous and particulate sulfur constituents, Journal of Geophysical Research-Atmospheres, 112, D15304

10.1029/2006jd007914, 2007a.

Karl, T. G., Christian, T. J., Yokelson, R. J., Artaxo, P., Hao, W. M., and Guenther, A.: The Tropical Forest and Fire Emissions Experiment: method evaluation of volatile organic compound emissions measured by PTR-MS, FTIR, and GC from tropical biomass burning, Atmospheric Chemistry and Physics, 7, 5883-5897, 2007b.

Keywood, M., Kanakidou, M., Stohl, A., Dentener, F., Grassi, G., Meyer, C. P., Torseth, K., Edwards, D., Thompson, A., Lohmann, U., and Burrows, J. P.: Fire in the Air- Biomass burning impacts in a changing climate, Critical Reviews in Environmental Science and Technology, DOI:10.1080/10643389.2011.604248 2011.

Kitchener, A., and Harris, S.: From Forest to Fjaeldmark: Descriptions of Tasmania's Vegetation, 2 ed., Department of Primary Industries, Parks, Water and Environment, Tasmania, 2013.

Kondo, Y., Matsui, H., Moteki, N., Sahu, L., Takegawa, N., Kajino, M., Zhao, Y., Cubison, M. J., Jimenez, J. L., Vay, S., Diskin, G. S., Anderson, B., Wisthaler, A., Mikoviny, T., Fuelberg, H. E., Blake, D. R., Huey, G., Weinheimer, A. J., Knapp, D. J., and Brune, W. H.: Emissions of black carbon, organic, and inorganic aerosols from biomass burning in North America and Asia in 2008, Journal of Geophysical Research-Atmospheres, 116, 10.1029/2010jd015152, 2011.

Korhonen, H., Carslaw, K. S., Spracklen, D. V., Mann, G. W., and Woodhouse, M. T.: Influence of oceanic dimethyl sulfide emissions on cloud condensation nuclei concentrations and seasonality over the remote Southern Hemisphere oceans: A global model study, Journal of Geophysical Research-Atmospheres, 113, D15204 10.1029/2007jd009718, 2008.

Krummel, P. B., Fraser, P., Steele, L. P., Porter, L. W., Derek, N., Rickard, C., Dunse, B. L., Langenfelds, R. L., Miller, B. R., Baly, S. B., and McEwan, S., The AGAGE in situ program for non-CO2 greenhouse gases at Cape Grim, 2005-2006: methane, nitrous oxide, carbon monoxide, hydrogen, CFCs, HCFCs, HFCs, PFCs, halons, chlorocarbons, hydrocarbons and sulphur hexafluoride, 2005-2006 Baseline Atmospheric Program (Australia), edited by: Cainey, J.M., Derek, N. and Krummel, P.B., Australian Bureau of Meteorology and CSIRO Marine and Atmospheric Research, 65-77, 2007, available at: http://www.bom.gov.au/inside/cgbaps/baseline/Baseline_2005-2006.pdf

Lawler, M. J., Whitehead, J., O'Dowd, C., Monahan, C., McFiggans, G., and Smith, J. N.: Composition of 15–85 nm particles in marine air, Atmos. Chem. Phys., 14, 11557-11569, 10.5194/acp-14-11557-2014, 2014.

Lawson, S. J., Cope, M., Lee, S., Keywood, M., Galbally, I. E., and Ristovski, Z.: Biomass Burning at Cape Grim: using modelling to explore plume photochemistry and composition, Atmos. Chem. Phys., 2015. In preparation.

Lewis, A. C., Evans, M. J., Hopkins, J. R., Punjabi, S., Read, K. A., Purvis, R. M., Andrews, S. J., Moller, S. J., Carpenter, L. J., Lee, J. D., Rickard, A. R., Palmer, P. I., and Parrington, M.: The influence of biomass burning on the global distribution of selected non-methane organic compounds, Atmospheric Chemistry and Physics, 13, 851-867, 10.5194/acp-13-851-2013, 2013.

Martin, M., Tritscher, T., Jurányi, Z., Heringa, M. F., Sierau, B., Weingartner, E., Chirico, R., Gysel, M., Prévôt, A. S. H., Baltensperger, U., and Lohmann, U.: Hygroscopic properties of fresh and aged wood burning particles, J. Aerosol. Sci., 56, 15-29, http://dx.doi.org/10.1016/j.jaerosci.2012.08.006, 2013.

May, A. A., McMeeking, G. R., Lee, T., Taylor, J. W., Craven, J. S., Burling, I., Sullivan, A. P., Akagi, S., Collett, J. L., Flynn, M., Coe, H., Urbanski, S. P., Seinfeld, J. H., Yokelson, R. J., and Kreidenweis, S. M.: Aerosol emissions from prescribed fires in the United States: A synthesis of laboratory and aircraft measurements, Journal of Geophysical Research: Atmospheres, 119, 11,826-811,849, 10.1002/2014JD021848, 2014.

McCulloch, A., Midgley, P. M., and Ashford, P.: Releases of refrigerant gases (CFC-12, HCFC-22 and HFC-134a) to the atmosphere, Atmospheric Environment, 37, 889-902, http://dx.doi.org/10.1016/S1352-2310(02)00975-5, 2003.

McKenzie, L. M., Ward, D. E., and Hao, W. M.: Chlorine and bromine in the biomass of tropical and temperate ecosystems, Biomass Burning and Global Change, vol. 1, Remote Sensing, Modeling and Inventory Development, and Biomass Burning in Africa, edited by: J.S., L., MIT Press, Cambridge, Massachusetts, 1996.

Meyer, C. P., Cook, G. D., Reisen, F., Smith, T. E. L., Tattaris, M., Russell-Smith, J., Maier, S., Yates, C. P., and Wooster, M. J.: Direct measurements of the seasonality of emission factors from savanna fires in northern Australia, Journal of Geophysical Research-Atmospheres, 117, 2012.

Meyer, C. P., and Cook, G. D.: Biomass combustion and emission processes in the Northern Australian Savannas, in: Carbon Accounting and Savanna Fire Management, edited by: Murphy, B. P., Edwards, A. C., Meyer, C. P., and Russell-Smith, J., CSIRO Publishing, Clayton Australia 185-234 2015.

Miller, B. R., Weiss, R. F., Salameh, P. K., Tanhua, T., Greally, B. R., Mühle, J., and Simmonds, P. G.: Medusa: A Sample Preconcentration and GC/MS Detector System for in Situ Measurements of Atmospheric Trace Halocarbons, Hydrocarbons, and Sulfur Compounds, Anal. Chem., 80, 1536-1545, 10.1021/ac702084k, 2008.

Ortega, A. M., Day, D. A., Cubison, M. J., Brune, W. H., Bon, D., de Gouw, J. A., and Jimenez, J. L.: Secondary organic aerosol formation and primary organic aerosol oxidation from biomass-burning smoke in a flow reactor during FLAME-3, Atmospheric Chemistry and Physics, 13, 11551-11571, 10.5194/acp-13-11551-2013, 2013.

Paton-Walsh, C., Jones, N. B., Wilson, S. R., Haverd, V., Meier, A., Griffith, D. W. T., and Rinsland, C. P.: Measurements of trace gas emissions from Australian forest fires and correlations with coincident measurements of aerosol optical depth, Journal of Geophysical Research-Atmospheres, 110, 10.1029/2005jd006202, 2005.

Paton-Walsh, C., Wilson, S. R., Jones, N. B., and Griffith, D. W. T.: Measurement of methanol emissions from Australian wildfires by ground-based solar Fourier transform spectroscopy, Geophysical Research Letters, 35, 5, L08810,10.1029/2007gl032951, 2008.

Paton-Walsh, C., Deutscher, N. M., Griffith, D. W. T., Forgan, B. W., Wilson, S. R., Jones, N. B., and Edwards, D. P.: Trace gas emissions from savanna fires in northern Australia, Journal of Geophysical Research-Atmospheres, 115, 12, D16314m 10.1029/2009jd013309, 2010.

Paton-Walsh, C., Emmons, L. K., and Wiedinmyer, C.: Australia's Black Saturday fires - comparison of techniques for estimating emissions from vegetation fires, Atmospheric Environment, 60, 262-270, 10.1016/j.atmosenv.2012.06.066, 2012.

Paton-Walsh, C., Smith, T. E. L., Young, E. L., Griffith, D. W. T., and Guérette, É. A.: New emission factors for Australian vegetation fires measured using open-path Fourier transform infrared spectroscopy – Part 1: methods and Australian temperate forest fires, Atmos. Chem. Phys. Discuss., 14, 4327-4381, 10.5194/acpd-14-4327-2014, 2014.

Petters, M. D., Carrico, C. M., Kreidenweis, S. M., Prenni, A. J., DeMott, P. J., Collett, J. L., and Moosmüller, H.: Cloud condensation nucleation activity of biomass burning aerosol, Journal of Geophysical Research: Atmospheres, 114, n/a-n/a, 10.1029/2009JD012353, 2009.

Pratt, K. A., Murphy, S. M., Subramanian, R., DeMott, P. J., Kok, G. L., Campos, T., Rogers, D. C., Prenni, A. J., Heymsfield, A. J., Seinfeld, J. H., and Prather, K. A.: Flight-based chemical characterization of biomass burning aerosols within two prescribed burn smoke plumes, Atmospheric Chemistry and Physics, 11, 12549-12565, 10.5194/acp-11-12549-2011, 2011.

Prinn, R. G., Weiss, R. F., Fraser, P. J., Simmonds, P. G., Cunnold, D. M., Alyea, F. N., O'Doherty, S., Salameh, P., Miller, B. R., Huang, J., Wang, R. H. J., Hartley, D. E., Harth, C., Steele, L. P., Sturrock, G., Midgley, P. M., and McCulloch, A.: A history of chemically and radiatively important gases in air deduced from ALE/GAGE/AGAGE, Journal of Geophysical Research: Atmospheres, 105, 17751-17792, 10.1029/2000JD900141, 2000.

Quinn, P. K., and Bates, T. S.: The case against climate regulation via oceanic phytoplankton sulphur emissions, Nature, 480, 51-56, 10.1038/nature10580, 2011.

Reinhardt, T. E., and Ward, D. E.: Factors Affecting Methyl Chloride Emissions from Forest Biomass Combustion, Environmental Science & Technology, 29, 825-832, 10.1021/es00003a034, 1995.

Sahu, L. K., Kondo, Y., Moteki, N., Takegawa, N., Zhao, Y., Cubison, M. J., Jimenez, J. L., Vay, S., Diskin, G. S., Wisthaler, A., Mikoviny, T., Huey, L. G., Weinheimer, A. J., and Knapp, D. J.: Emission characteristics of black carbon in anthropogenic and biomass burning plumes over California during ARCTAS-CARB 2008, Journal of Geophysical Research-Atmospheres, 117, 10.1029/2011jd017401, 2012.

Shirai, T., Blake, D. R., Meinardi, S., Rowland, F. S., Russell-Smith, J., Edwards, A., Kondo, Y., Koike, M., Kita, K., Machida, T., Takegawa, N., Nishi, N., Kawakami, S., and Ogawa, T.: Emission estimates of selected volatile organic compounds from tropical savanna burning in northern Australia, Journal of Geophysical Research-Atmospheres, 108, 10.1029/2001jd000841, 2003.

Simpson, I. J., Akagi, S. K., Barletta, B., Blake, N. J., Choi, Y., Diskin, G. S., Fried, A., Fuelberg, H. E., Meinardi, S., Rowland, F. S., Vay, S. A., Weinheimer, A. J., Wennberg, P. O., Wiebring, P., Wisthaler, A., Yang, M., Yokelson, R. J., and Blake, D. R.: Boreal forest fire emissions in fresh Canadian smoke plumes: C(1)-C(10) volatile organic compounds (VOCs), CO(2), CO, NO(2), NO, HCN and CH(3)CN, Atmospheric Chemistry and Physics, 11, 6445-6463, 10.5194/acp-11-6445-2011, 2011.

Smith, T. E. L., Paton-Walsh, C., Meyer, C. P., Cook, G. D., Maier, S. W., Russell-Smith, J., Wooster, M. J., and Yates, C. P.: New emission factors for Australian vegetation fires measured using open-path Fourier transform infrared spectroscopy – Part 2: Australian tropical savanna fires, Atmos. Chem. Phys. Discuss., 14, 6311-6360, 10.5194/acpd-14-6311-2014, 2014.

Steele, L. P., Krummel, P. B., Spencer, D. A., Rickard, C., Baly, S. B., Langenfelds, R. L., and van der Schoot, M. V., http://www.bom.gov.au/inside/cgbaps/baseline.shtml Baseline carbon dioxide monitoring, in: Baseline Atmospheric Program Australia 2005-2006, Baseline Atmospheric Program Australia 2005-2006, 2007.

Stockwell, C. E., Yokelson, R. J., Kreidenweis, S. M., Robinson, A. L., DeMott, P. J., Sullivan, R. C., Reardon, J., Ryan, K. C., Griffith, D. W. T., and Stevens, L.: Trace gas emissions from combustion of peat, crop residue, domestic biofuels, grasses, and other fuels: configuration and Fourier transform infrared (FTIR) component of the fourth Fire Lab at Missoula Experiment (FLAME-4), Atmospheric Chemistry and Physics, 14, 9727-9754, 10.5194/acp-14-9727-2014, 2014.

Stockwell, C. E., Veres, P. R., Williams, J., and Yokelson, R. J.: Characterization of biomass burning emissions from cooking fires, peat, crop residue, and other fuels with high-resolution proton-transfer-reaction time-of-flight mass spectrometry, Atmos. Chem. Phys., 15, 845-865, 10.5194/acp-15-845-2015, 2015.

Vakkari, V., Kerminen, V.-M., Beukes, J. P., Tiitta, P., van Zyl, P. G., Josipovic, M., Venter, A. D., Jaars, K., Worsnop, D. R., Kulmala, M., and Laakso, L.: Rapid changes in biomass burning aerosols by atmospheric oxidation, Geophysical Research Letters, 41, 2014GL059396, 10.1002/2014GL059396, 2014.

van Leeuwen, T. T., and van der Werf, G. R.: Spatial and temporal variability in the ratio of trace gases emitted from biomass burning, Atmospheric Chemistry and Physics, 11, 3611-3629, 10.5194/acp-11-3611-2011, 2011.

Volkova, L., Meyer, C. P., Murphy, S., Fairman, T., Reisen, F., and Weston, C.: Fuel reduction burning mitigates wildfire effects on forest carbon and greenhouse gas emission, International Journal of Wildland Fire, 23, 771-780, http://dx.doi.org/10.1071/WF14009, 2014.

Vollmer, M. K., Walter, S., Mohn, J., Steinbacher, M., Bond, S. W., Röckmann, T., and Reimann, S.: Molecular hydrogen (H2) combustion emissions and their isotope (D/H) signatures from domestic heaters, diesel vehicle engines, waste incinerator plants, and biomass burning, Atmos. Chem. Phys., 12, 6275-6289, 10.5194/acp-12-6275-2012, 2012.

Ward, D. E., and Radke, L. F.: Emission measurements from vegetation fires: A comparative evaluation of methods and results, in: Fire in the Environment: The Ecological, Atmospheric, and Climatic Importance of Vegetation Fires John Wiley & Sons Ltd., 1993

Watson, J. G., Chow, J. C., Chen, L. W. A., Lowenthal, D. H., Fujita, E. M., Kuhns, H. D., Sodeman, D. A., Campbell, D. E., Moosmüller, H., Zhu, D., and Motallebi, N.: Particulate emission factors for mobile fossil fuel and biomass combustion sources, Sci. Total Environ., 409, 2384-2396, http://dx.doi.org/10.1016/j.scitotenv.2011.02.041, 2011.

Wigder, N. L., Jaffe, D. A., and Saketa, F. A.: Ozone and particulate matter enhancements from regional wildfires observed at Mount Bachelor during 2004-2011, Atmospheric Environment, 75, 24-31, 10.1016/j.atmosenv.2013.04.026, 2013.

Yokelson, R. J., Goode, J. G., Ward, D. E., Susott, R. A., Babbitt, R. E., Wade, D. D., Bertschi, I., Griffith, D. W. T., and Hao, W. M.: Emissions of formaldehyde, acetic acid, methanol, and other trace gases from biomass fires in North Carolina measured by airborne Fourier transform infrared spectroscopy, Journal of Geophysical Research-Atmospheres, 104, 30109-30125, 10.1029/1999jd900817, 1999.

Yokelson, R. J., Bertschi, I. T., Christian, T. J., Hobbs, P. V., Ward, D. E., and Hao, W. M.: Trace gas measurements in nascent, aged, and cloud-processed smoke from African savanna fires by airborne Fourier transform infrared spectroscopy (AFTIR), Journal of Geophysical Research-Atmospheres, 108, 8478 10.1029/2002jd002322, 2003.

Yokelson, R. J., Urbanski, S. P., Atlas, E. L., Toohey, D. W., Alvarado, E. C., Crounse, J. D., Wennberg, P. O., Fisher, M. E., Wold, C. E., Campos, T. L., Adachi, K., Buseck, P. R., and Hao, W. M.: Emissions from forest fires near Mexico City, Atmos. Chem. Phys., 7, 5569-5584, 10.5194/acp-7-5569-2007, 2007.Yokelson, R. J., Crounse, J. D., DeCarlo, P. F., Karl, T., Urbanski, S., Atlas, E., Campos, T., Shinozuka, Y., Kapustin, V., Clarke, A. D., Weinheimer, A., Knapp, D. J., Montzka, D. D., Holloway, J., Weibring, P., Flocke, F., Zheng, W., Toohey, D., Wennberg, P. O., Wiedinmyer, C., Mauldin, L., Fried, A., Richter, D., Walega, J., Jimenez, J. L., Adachi, K., Buseck, P. R., Hall, S. R., and Shetter, R.:

Emissions from biomass burning in the Yucatan, Atmospheric Chemistry and Physics, 9, 5785-5812, 2009.

Yokelson, R. J., Burling, I. R., Gilman, J. B., Warneke, C., Stockwell, C. E., de Gouw, J., Akagi, S. K., Urbanski, S. P., Veres, P., Roberts, J. M., Kuster, W. C., Reardon, J., Griffith, D. W. T., Johnson, T. J., Hosseini, S., Miller, J. W., Cocker, D. R., Jung, H., and Weise, D. R.: Coupling field and laboratory measurements to estimate the emission factors of identified and unidentified trace gases for prescribed fires, Atmospheric Chemistry and Physics, 13, 89-116, 10.5194/acp-13-89-2013, 2013.

1 Tab01

Measurement	Instrument	Air intake height	Time resolution	Reference
NMOCs	PTR-MS	10m	10 min	(Galbally et al., 2007a)
Particle size distribution and number 14-700 nm	SMPS	10m	1 min	(Cravigan et al., 2015)
Condensation nuclei (particle number > 3 nm)	TSI particle counters	10m	1 min	(Gras, 2007)
black carbon concentration	aethelometer	10m	integrated 30 min	(Gras, 2007)
CCN number at 0.5% SS	CCN counter	10m	1 min	(Gras, 2007)
ozone (O_3)	TECO analyser	10m	1 min	(Galbally et al., 2007b)
methane (CH_4)	AGAGE GC-FID	10m/70m/75m	40 min (discrete air sample every 40 minutes)	(Prinn et al., 2000; Krummel et al., 2007)
carbon monoxide (CO) and hydrogen (H_2)	AGAGE GC-MRD	10m/70m/75m	40 min (discrete air sample every 40 minutes)	(Prinn et al., 2000; Krummel et al., 2007)
carbon dioxide (CO_2)	CSIRO LoFlo NDIR	70m	1 min (continuous analyser)	(Steele et al., 2007)
nitrous oxide (N_2O), major CFCs, $CHCl_3$, CH_3CCl_3, CCl_4	AGAGE GC-ECD system	10m/70m/75m	40 min (discrete air sample every 40 minutes)	(Prinn et al., 2000; Krummel et al., 2007)
minor CFCs, HCFCs, HFCs, PFCs, methylhalides, chlorinated solvents, halons, ethane	AGAGE GC-MS-Medusa	75m	2 hour (20 minute integrated air sample every 2 hours)	(Miller et al., 2008; Prinn et al., 2000; Krummel et al., 2007)

Tab02

Event	Date and Time	Period	Air Mass Origin	Marker Species	Comments
BB 1	16/02/2006 2:00	A	Ocean & NW Tasmania	CO, BC, low O_3, particles (uni modal)	Fresh Plume
	16/02/2006 6:00	B	Ocean & NW Tasmania	BC, O_3, particle growth	Particle growth
	16/02/2006 12:00	C	mainland Australia	O_3 (overnight enhancement)	Background terrestrial
	17/02/2006 6:00	D	Melbourne	O_3, particles, HFC-134a	Urban
	17/02/2006 15:00	E	Ocean	Particles (bi-modal)	Clean Marine
	18/02/2006 0:00	F	Ocean & mainland Australia	O_3, HFC-134a	Marine with minor terrestrial
BB2	23/02/2006 23:00	A	Ocean & NW Tasmania	CO, BC, Acetonitrile, particles	Fresh Plume
	24/02/2006 23:00	B	mainland Australia	CO, NMOC (Acetonitrile)	Fresh plume + precipitation
	25/02/2006 5:00	C	Melbourne	HFC-134a, O_3	Urban
	25/02/2006 23:00	D	Ocean	Low particles, HFC-134a	Clean Marine

Tab03

Compound	formula	Background concentration[a]	BB plume concentration[a]	ER CO[b]	CO ER R^2	EF (g kg^{-1})[c]
Species statistically enhanced in plume		mean (stdev)	mean (stdev)			
carbon dioxide	CO_2	378.1 (0.7)	382.9 (1.2)	1620	0.15	1621
carbon monoxide	CO	42 (6)	618 (279)	n/a	n/a	127
methane	CH_4	1713 (2)	1743 (10)	49	0.48	3.8
nitrous oxide	N_2O	319.0 (0.2)	319.1 (0.2)	0.27	0.01	0.06
hydrogen	H_2	551 (3)	6010 (28)	100	0.87	0.93
ethane	C_2H_6	1845 (146)	1765 (1008)	3.2	0.79	0.41
hydrogen cyanide (m/z 28)	HCN	122 (4)	903 (292)	5.7	0.42	0.73
formaldehyde (m/z 31)	HCHO	541 (339)	1895 (561)	11	0.08	1.64
methanol (m/z 33)	CH_3OH	721 (413)	8603 (2521)	14	0.43	2.07
acetonitrile (m/z 42)	C_2H_3N	35 (4)	983 (324)	1.3	0.58	0.25
acetaldehyde (m/z 45)	CH_3CHO	48 (27)	2608 (807)	4.4	0.53	0.92
unknown (m/z 46)	unknown	105 (72)	279 (74)	0.27	-0.9	0.06
formic acid (m/z 47)	CH_2O_2	19 (7)	141 (63)	0.20	-0.09	0.05
acetone/propanal (m/z 59)	C_3H_6O	170 (31)	1315 (372)	2.0	0.40	0.54
acetic acid (m/z 61)	CH_3COOH	75 (32)	2054 (971)	3.6	0.64	0.75

furan/isoprene (m/z 69)	C_4H_4O	78 (39)	3113 (1139)	5.3	0.72	1.69
MVK/MAK (m/z 71)	C_4H6O	14 (10)	673 (234)	1.2	0.76	0.38
methylglyoxal/methyl ethyl ketone (m/z 73)	C_4H_8O	21 (12)	618 (209)	1.0	0.69	0.35
benzene (m/z 79)	C_6H_6	7 (6)	1093 (390)	1.9	0.78	0.69
2-furanone (m/z 85)	$C_4H_4O_2$	15 (5)	847 (276)	1.5	0.51	0.57
2,3-butanedione (m/z 87)	$C_4H_6O_2$	16 (5)	576 (186)	0.97	0.67	0.39
toluene (m/z 93)	C_7H_8	8 (5)	409 (113)	0.69	0.51	0.30
phenol (m/z 95)	C_6H_5OH	12 (9)	472 (149)	0.80	0.73	0.35
unknown (m/z 101)	Unknown	15 (4)	124 (33)	0.19	0.32	0.09
xylenes (m/z 107)	C_8H_{10}	15 (0)	319 (100)	0.53	0.70	0.26
unknown (m/z 113)	unknown	9 (0)	279 (87)	0.47	0.60	0.25
C_3-benzenes (m/z 121)	C_9H_{12}	20 (12)	290 (89)	0.47	0.73	0.27
monoterpenes + unknowns (m/z 137)	$C_{10}H_{16}/C_8H_8O_2$	17 (9)	219 (79)	0.18	0.51	0.11
unknown (m/z 153)	unknown	45 (135)	91 (29)	0.09	0.61	0.06
methyl chloride	CH_3Cl	594 (79)	1251 (458)	1.30	0.74	0.28
methyl bromide	CH_3Br	9 (2)	34 (18)	0.05	0.74	0.02
methyl iodide	CH_3I	1.3 (0.2)	3.7 (1.5)	0.004	0.75	0.002
black carbon	n/a	1.6 (0.3)	1657 (769)	0.003	0.81	0.16
CN > 3 nm	n/a	625 (2078)	24902 (8031)	38.4	0.7	n/a

CCN 0.5%	n/a	160 (31)	5501 (1355)	8.3	-0.4	n/a
Species not statistically enhanced in plume						
dimethyl sulphide (m/z 63)	C_2H_6S	158 (57)	172 (15)	n/a	n/a	n/a
chloroform	$CHCl_3$	6.6 (0.5)	8.8 (1.4)	n/a	n/a	n/a
methyl chloroform	CH_3CCl_3	16.1 (0.2)	16.0 (0.2)	n/a	n/a	n/a
dichloromethane	CH_2Cl_2	7.5 (0.04)	7.6 (0.1)	n/a	n/a	n/a
carbon tetrachloride	CCl_4	90.2 (0.7)	90.3 (0.2)	n/a	n/a	n/a
bromoform	$CHBr_3$	4.2 (0.8)	4.7 (0.4)	n/a	n/a	n/a
HFC-32	CH_2F_2	1.02 (0.03)	1.04 (0.03)	n/a	n/a	n/a
HFC-125	C_2HF_5	3.57 (0.04)	3.63 (0.05)	n/a	n/a	n/a
HFC-134a	CH_2FCF_3	33.20 (0.22)	33.28 (0.17)	n/a	n/a	n/a
ozone	O_3	15.1 (1.1)	15.8 (1.5)	n/a	n/a	n/a

Tab04

	This study g kg^{-1} (coastal heath)	Temperate south eastern Australia	Tropical savannah Australia	Temperate Northern Hemisphere
Hydrogen (H_2)	0.93	n/a	n/a	2.03 (1.79) [j]
Methane (CH_4)	3.8	3.5 (1.1) [c]	2.26 (1.27) [d] 2.33 (0.80) [e] 2.20 (0.32) [f] 2.03 (0.13) [h] 2.10 (1.16) [i]	3.92 (2.39) [j] 3.69 (1.36) [l]
Ethane (C_2H_6)	0.41	0.26 (0.11) [a] 0.5 (0.2) [c]	0.60 (0.225) [d] 0.11 (0.09) [e] 0.53 (0.02) [f] 0.13 (0.04) [g] 0.08 (0.05) [i]	1.12 (0.67) [j] 0.48 (0.61) [l]
Hydrogen cyanide (HCN)	0.73	0.43 (0.22)[a]	0.036 (0.002) [d] 0.025 (0.024) [e] 0.11 (0.04) [g] 0.53 (0.31) [i]	0.73 (0.19) [j] 0.75 (0.26) [l]
Acetonitrile (CH_3CN)	0.25	n/a	0.11 (0.06) [f]	0.15 (0.07) [l]
Acetaldehyde (C_2H_4O)	0.92	n/a	0.55 (0.26) [d] 1.0 (0.62) [e]	0.56 (0.40)[l]
Phenol (C_6H_5OH)	0.35	n/a	n/a	0.33 (0.38) [j]

				0.45 (0.19) [l]
Acetic acid (CH_3COOH)	0.75	3.8 (1.3)[c]	1.54 (0.64) [i]	1.97 (1.66) [j] 1.91 (0.93) [l]
Methanol (CH_3OH)	2.07	2.3 (0.8)[b] 2.4 (1.2)[c]	1.06 (0.87) [i]	1.93 (1.38)[j] 1.35 (0.4) [l]
Benzene (C_6H_6)	0.69	n/a	0.42 (0.23) [d] 0.29 (0.24) [e] 0.21 (0.02) [f]	0.45 (0.29) [l]
Toluene (C_7H_8)	0.30	n/a	n/a	0.17 (0.13) [l]
Methyl chloride (CH_3Cl)	0.28	n/a	0.0605 (0.0072) [f]	0.059[k]
Methyl bromide (CH_3Br)	0.02	n/a	0.0018 (0.0003)f	0.0036[k]
Methyl iodide(CH_3I)	0.002	n/a	n/a	0.0008[k]

Table 1. Measurement summary

Table 2. Summary of Periods described in the text for BB1 and BB2 (as shown in Figs 3 and 6)

Table 3. Summary of species measured in BB2 coastal heathland fire including background concentration, plume concentration, ER to CO and EF. [a] Units – all in ppt except for CO, CH_4, N_2O in ppb, CO_2 in ppm, CN and CCN in particles cm^{-3}, BC in ng m^{-3} [b]Trace gas emission ratios are molar ratios, BC is mass ratio, particle number is # particles ppb^{-1} [c] calculated using carbon mass balance method n/a = not applicable

Table 4. Comparison of emission factors with other studies

[a] Paton-Walsh et al., 2005, [b] Paton-Walsh et al., 2008, [c] Paton-Walsh et al., 2014, [d]Hurst et al., 1994a [e]Hurst et al., 1994b [f] Shirai et al., 2003 [g] Paton-Walsh et al., 2010 [h] Meyer et al., 2012 [i] Smith et al., 2014 [j]Akagi et al., 2011 temperate updated May 2014 [k]Akagi et al., 2011 extratropical [l]Yokelson et al., 2013 semi arid shrubland

Fig 01

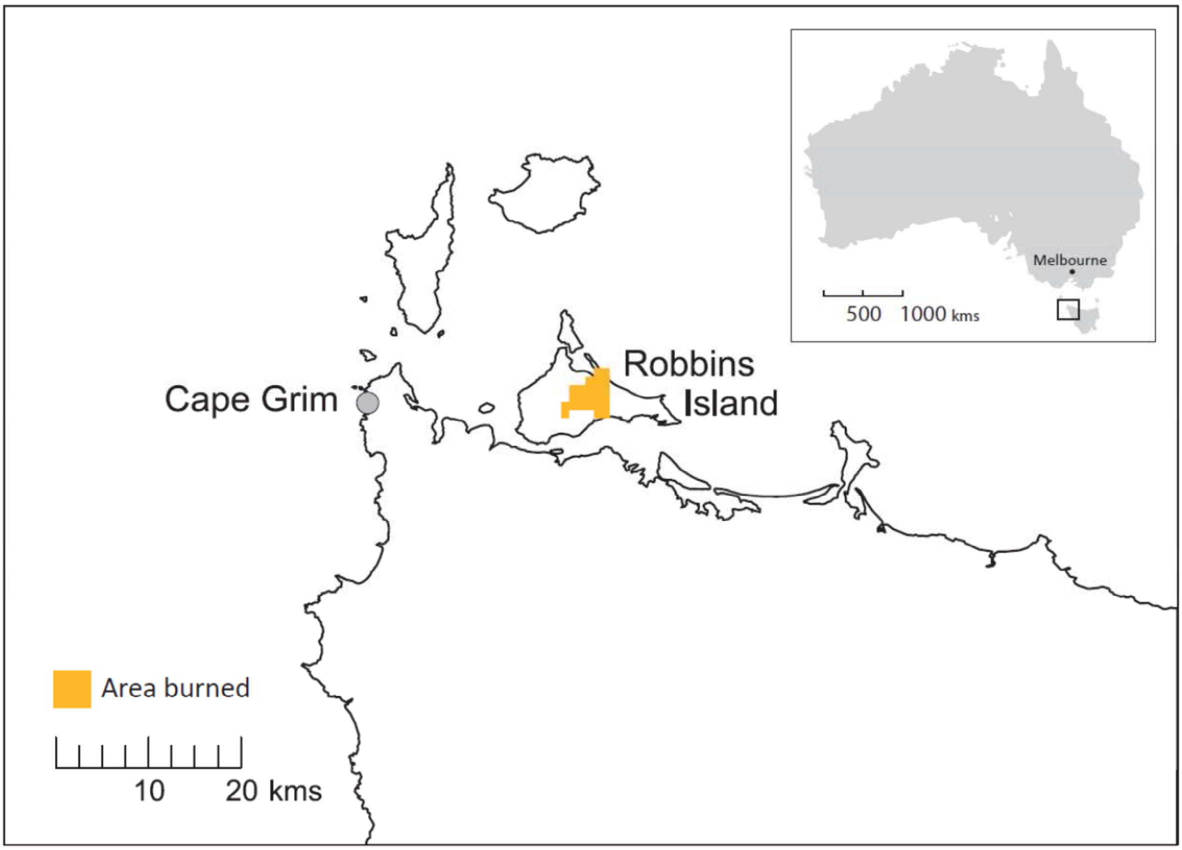

Fig 02

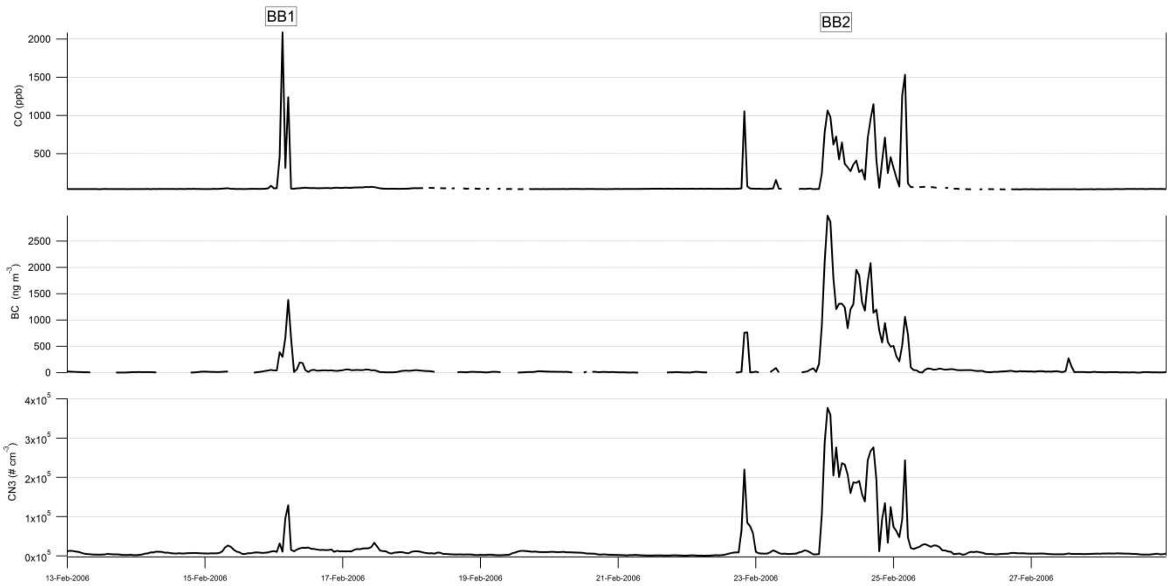

Fig 03

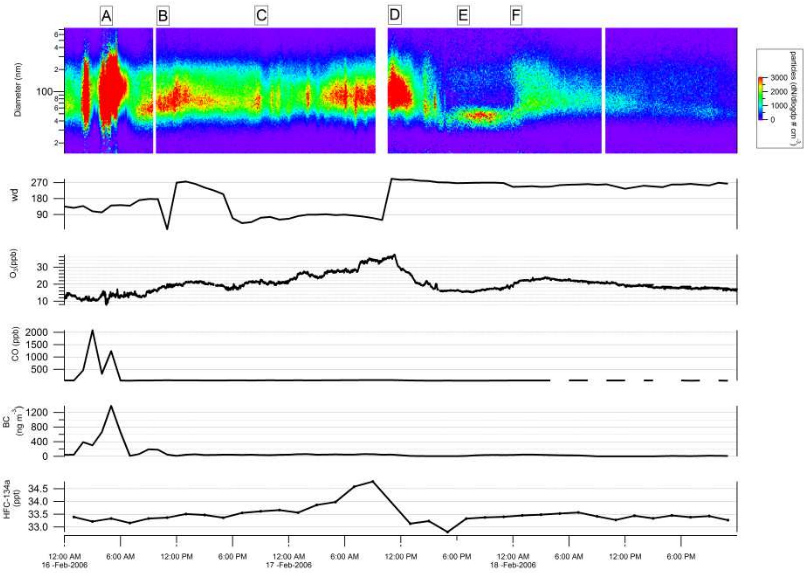

Fig 04

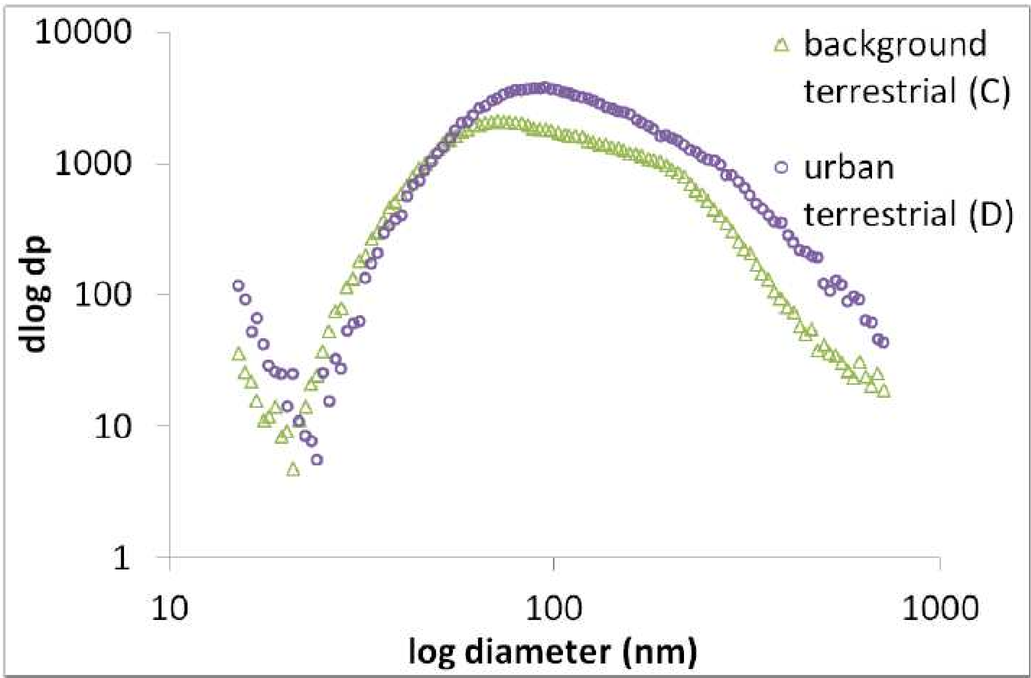

Fig04b

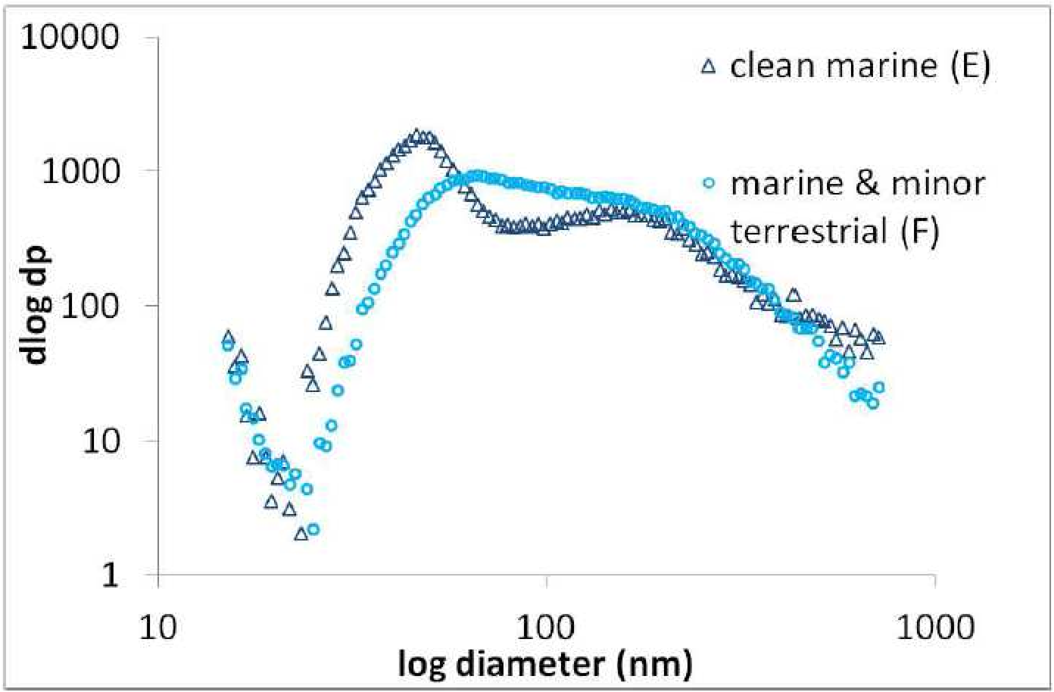

Fig 04c

Fig 05

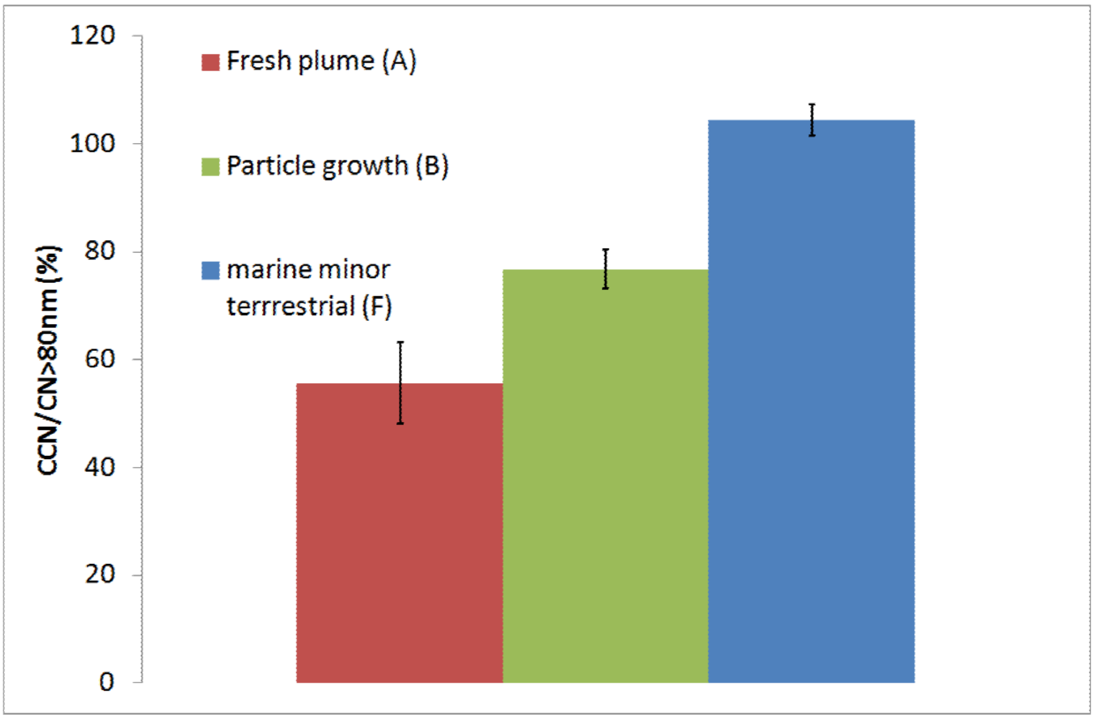

Fig05a

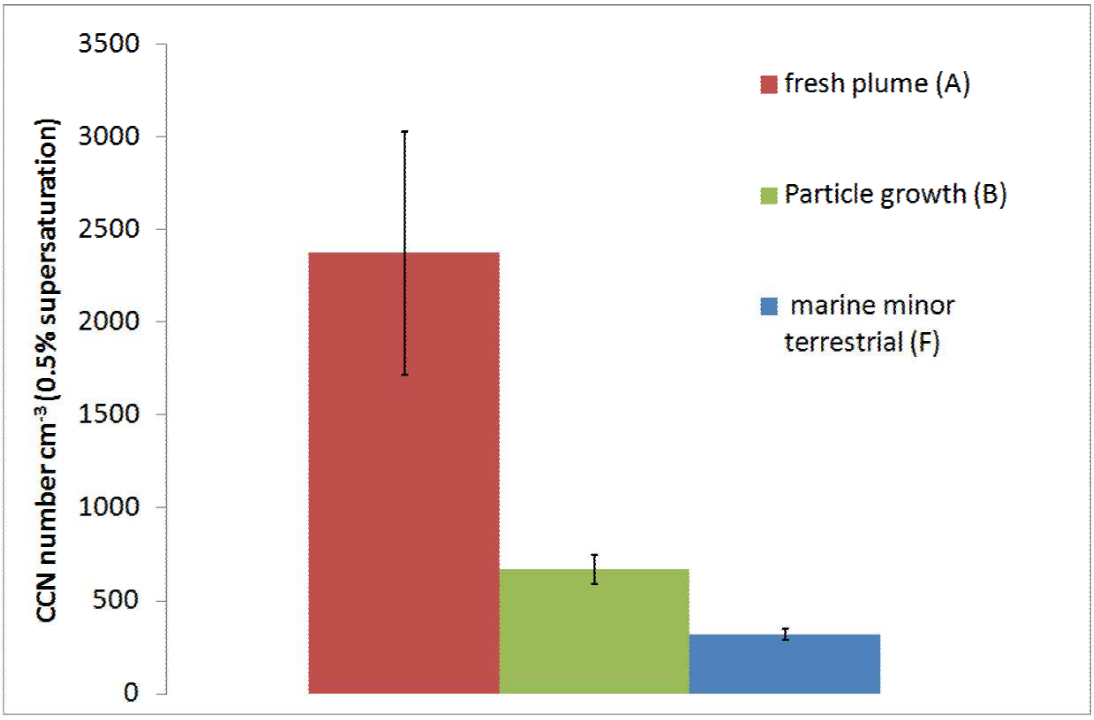

Fig05b

Fig 06

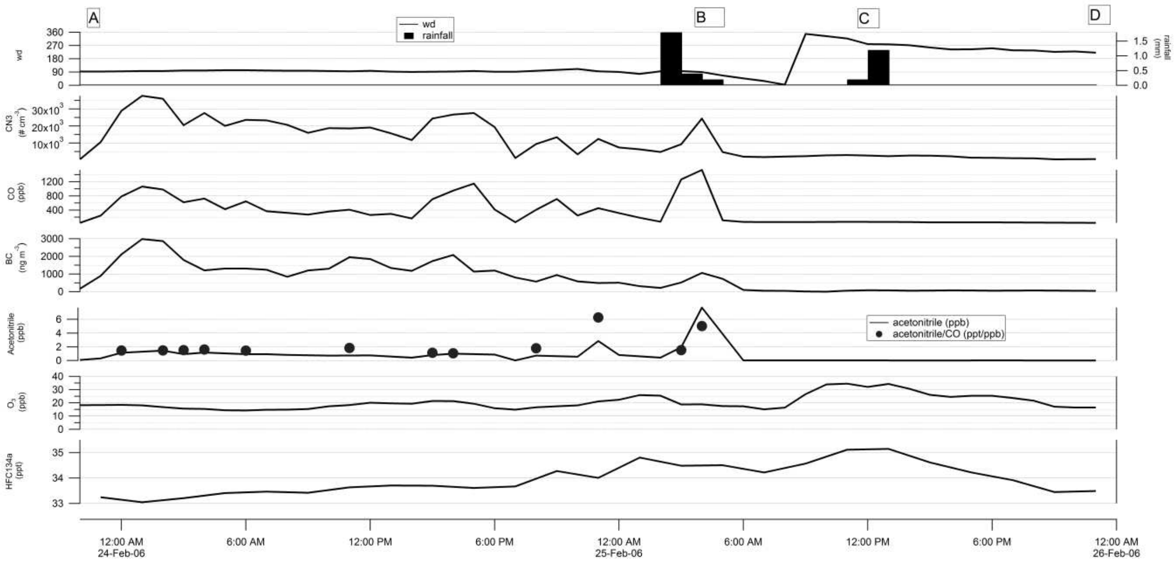

Fig 07

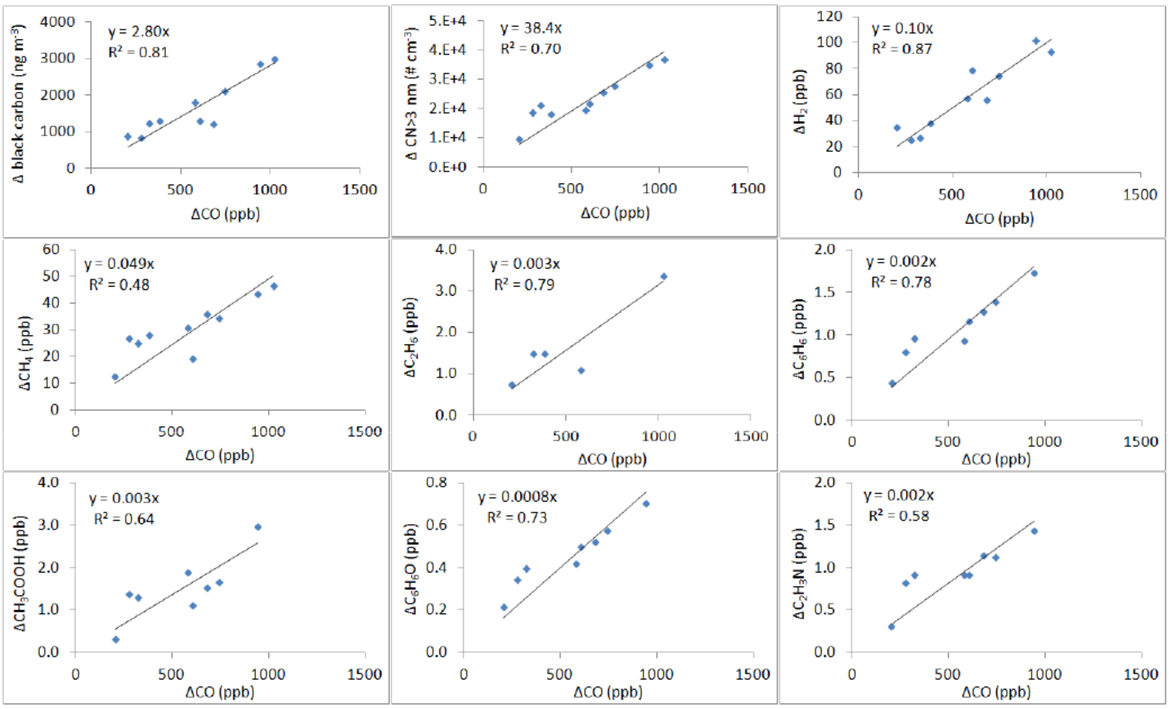

Figure 1. Location of Cape Grim and Robbins Island in North West Tasmania, Australia. Area burned is shown.

Figure 2. Time series of carbon monoxide (CO), black carbon (BC) and particles>3 nm (CN3) for the study period (BB 1 and BB2 shown).

Figure 3. Time series from BB1 including a particle size and number contour plot, wind direction (degrees), ozone (O_3), carbon monoxide (CO), black carbon (BC) and HFC-134a. Periods A-F are discussed in the text.

Figure 4. Average particle size distributions (with log scale on both axes) from BB1 corresponding to periods shown in Fig 3 including (a) the fresh plume (Period A) and particle growth (Period B) (b) background terrestrial (Period C) and urban terrestrial (Period D) and (c) clean marine (Period E) and marine and minor terrestrial (Period F).

Figure 5 (a) Average ratios of CCN/CN>80 (hourly) in BB1 during fresh plume (Fig 3. Period A), particle growth event (Fig. 3 Period B), and in marine air with minor terrestrial influence (Fig 3. Period F). (b) average absolute number concentrations of CCN (hourly) during the same periods. Error bars are one standard error of the mean

Figure 6. Time series from BB2 including wind direction and rainfall, CN3 (particle number > 3 nm), CO (carbon monoxide), BC (black carbon), acetonitrile and ratio of acetonitrile to CO, O_3 and HFC-134a. Events corresponding to Periods A–D are discussed in the text.

Figure 7. Emission ratios (ER) of several trace gas and aerosol species to CO during Period A in BB2